

AD-A160 375 SOME MICROPHYSICAL PROCESSES AFFECTING AIRCRAFT ICING 1/1
(U) AIR FORCE GEOPHYSICS LAB HANSCOM AFB MA
H J SWEENEY ET AL. 08 MAY 85 AFGL-TR-85-0100

AD-A160 375 SOME MICROPHYSICAL PROCESSES AFFECTING AIRCRAFT ICING 1/1
(U) AIR FORCE GEOPHYSICS LAB HANSCOM AFB MA
H J SWEENEY ET AL. 08 MAY 85 AFGL-TR-85-0100

AD-A160 375 SOME MICROPHYSICAL PROCESSES AFFECTING AIRCRAFT ICING 1/1
(U) AIR FORCE GEOPHYSICS LAB HANSCOM AFB MA
H J SWEENEY ET AL. 08 MAY 85 AFGL-TR-85-0100

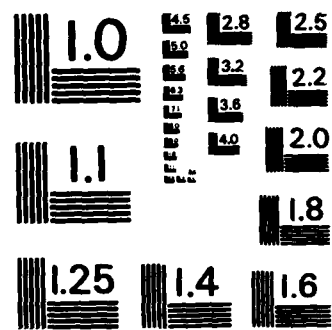
AD-A160 375 SOME MICROPHYSICAL PROCESSES AFFECTING AIRCRAFT ICING 1/1
(U) AIR FORCE GEOPHYSICS LAB HANSCOM AFB MA
H J SWEENEY ET AL. 08 MAY 85 AFGL-TR-85-0100

AD-A160 375 SOME MICROPHYSICAL PROCESSES AFFECTING AIRCRAFT ICING 1/1
(U) AIR FORCE GEOPHYSICS LAB HANSCOM AFB MA
H J SWEENEY ET AL. 08 MAY 85 AFGL-TR-85-0100

AD-A160 375 SOME MICROPHYSICAL PROCESSES AFFECTING AIRCRAFT ICING 1/1
(U) AIR FORCE GEOPHYSICS LAB HANSCOM AFB MA
H J SWEENEY ET AL. 08 MAY 85 AFGL-TR-85-0100

AD-A160 375 SOME MICROPHYSICAL PROCESSES AFFECTING AIRCRAFT ICING 1/1
(U) AIR FORCE GEOPHYSICS LAB HANSCOM AFB MA
H J SWEENEY ET AL. 08 MAY 85 AFGL-TR-85-0100

[illegible][illegible][illegible]



MICROCOPY RESOLUTION TEST CHART
NATIONAL BUREAU OF STANDARDS - 1963 - A

AD-A160 375

Some Microphysical Processes Affecting Aircraft Icing — Final Report

HUGH J. SWEENEY
IAN D. COHEN, Capt, USAF



8 May 1985



Approved for public release; distribution unlimited.

DTIC
ELECTE
OCT 16 1985
S B D

DTIC FILE COPY



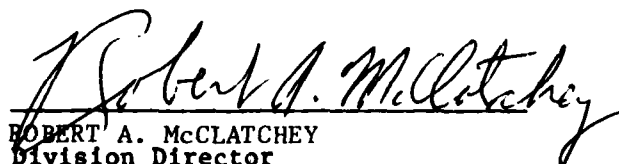
ATMOSPHERIC SCIENCES DIVISION
AIR FORCE GEOPHYSICS LABORATORY
PROJECT 6670
HANSCOM AFB, MA 01731

85 10 16 126

"This technical report has been reviewed and is approved for publication"

FOR THE COMMANDER


ARNOLD A. BARNES, Jr.
Branch Chief


ROBERT A. McCLATCHEY
Division Director

This document has been reviewed by the ESD Public Affairs Office (PA) and is releasable to the National Technical Information Service (NTIS).

Qualified requestors may obtain additional copies from the Defense Technical Information Center. All others should apply to the National Technical Information Service.

If your address has changed, or if you wish to be removed from the mailing list, or if the addressee is no longer employed by your organization, please notify AFGL/DAA/LYC Hanscom AFB, MA 01731. This will assist us in maintaining a current mailing list.

Unclassified

SECURITY CLASSIFICATION OF THIS PAGE

REPORT DOCUMENTATION PAGE				
1a. REPORT SECURITY CLASSIFICATION Unclassified		1b. RESTRICTIVE MARKINGS		
2a. SECURITY CLASSIFICATION AUTHORITY		3. DISTRIBUTION/AVAILABILITY OF REPORT Approved for public release, distribution unlimited.		
2b. DECLASSIFICATION/DOWNGRADING SCHEDULE				
4. PERFORMING ORGANIZATION REPORT NUMBER(S) AFGL-TR-85-0100 ERP, No. 914		5. MONITORING ORGANIZATION REPORT NUMBER(S)		
6a. NAME OF PERFORMING ORGANIZATION Air Force Geophysics Laboratory	6b. OFFICE SYMBOL (If applicable) LYC	7a. NAME OF MONITORING ORGANIZATION Air Force Geophysics Laboratory		
6c. ADDRESS (City, State and ZIP Code) Hanscom AFB Massachusetts 01731		7b. ADDRESS (City, State and ZIP Code) Hanscom AFB Massachusetts 01731		
8a. NAME OF FUNDING/SPONSORING ORGANIZATION Air Force Geophysics Laboratory	8b. OFFICE SYMBOL (If applicable) LYC	9. PROCUREMENT INSTRUMENT IDENTIFICATION NUMBER		
8c. ADDRESS (City, State and ZIP Code) Hanscom AFB Massachusetts 01731		10. SOURCE OF FUNDING NOS.		
		PROGRAM ELEMENT NO.	PROJECT NO.	TASK NO.
		62101F	6670	12
11. TITLE (Include Security Classification) Some Microphysical Processes Affecting Aircraft Icing - Final Report		12. PERSONAL AUTHOR(S) Hugh J. Sweeney and Ian D. Cohen, Capt, USAF		
13a. TYPE OF REPORT Scientific, Final.	13b. TIME COVERED FROM 1 Oct 81 to 30 Sep 84	14. DATE OF REPORT (Yr, Mo., Day) 1985 May 8	15. PAGE COUNT 46	
16. SUPPLEMENTARY NOTATION Aircraft Icing System				
17. COSATI CODES		18. SUBJECT TERMS (Continue on reverse if necessary and identify by block number)		
FIELD	GROUP	SUB GR		
0402			Aircraft icing Cloud physics Particle distribution Aviation meteorology	
19. ABSTRACT (Continue on reverse if necessary and identify by block number) This report summarizes work done as part of the Aircraft Icing Probabilities program, including sections not previously published. It contains a look at icing in layer-type clouds, a comparison of (PMS) 2-D data from two flights, and a look at additional data obtained from researchers in the Federal Republic of Germany. The parameters measured in a warm and cold layer-type cloud near Peoria, Illinois are analyzed and compared. Liquid water content (LWC), cloud depth, particle diameter and particle concentration are compared. Variations of these parameters are compared. In mature clouds, where droplet sizes are approximately equal, the LWC is directly related to the number concentration. The icing rate, LWC and droplet size all increase as a function of height above cloud base. Synoptic patterns and PMS 2-D data obtained on two flights are compared. The first flight, made near Greensboro, North Carolina, was in an area of heavy precipitation. The large particles present produced very little icing. The other flight, near (Contd)				
20. DISTRIBUTION/AVAILABILITY OF ABSTRACT UNCLASSIFIED/UNLIMITED <input checked="" type="checkbox"/> SAME AS RPT <input type="checkbox"/> DTIC USERS <input type="checkbox"/>		21. ABSTRACT SECURITY CLASSIFICATION Unclassified		
22a. NAME OF RESPONSIBLE INDIVIDUAL Hugh J. Sweeney		22b. TELEPHONE NUMBER (Include Area Code) (617) 861-2943	22c. OFFICE SYMBOL LYC	

DD FORM 1473, 83 APR

EDITION OF 1 JAN 73 IS OBSOLETE

Unclassified
SECURITY CLASSIFICATION OF THIS PAGE

Unclassified

SECURITY CLASSIFICATION OF THIS PAGE

19. (Contd) -> Flint, MI -

Flint, Michigan, was in an area which was experiencing only spotty precipitation. The aircraft, however, experienced moderate icing.

Data gathered on aircraft observations in the Federal Republic of Germany are examined. The data show that in strong icing situations, there are many particles with diameters of 10 to 20 μm . The results match those obtained by our research flights.

↑
micrometers

Project: Cloud physics;
Aircraft not available,
Particle distribution
-21

Unclassified

SECURITY CLASSIFICATION OF THIS PAGE

Preface

This report summarizes recent research in aircraft icing done at the Air Force Geophysics Laboratory. The authors gratefully acknowledge the assistance of those personnel at the Cloud Physics Branch of AFGL and the 4950th Test Wing at Wright-Patterson AFB, Ohio, who participated in the flight program which provided much of the data upon which the research presented in this report is based. We are also indebted to the German Flight Test Facility, a part of the Federal Office of Military Technology and Procurement of the Federal Republic of Germany, for providing us with data taken by their DO-28 aircraft. Lt Col Peter Soliz of the European Office of Aerospace Research and Development (EOARD), of the Air Force office of Scientific Research (AFOSR) was instrumental in obtaining these data for us. Peter Miller, Andrew Menezies and D. Keith Roberts, of Digital Programming Services, Inc. provided computer generated products used in this study. We wish to thank Mr. Morton Glass and Dr. Arnold Barnes, Jr. for reviewing the manuscript and providing many helpful suggestions. Ms. Barbara Main drafted the line drawings and Mrs. Carolyn Fadden typed the manuscript.

DTIC
ELECTE
S **D**
OCT 16 1985

B —



iii

Accession For	
NTIS GRA&I	<input checked="checked" type="checkbox"/>
DTIC TAB	<input type="checkbox"/>
Unannounced	<input type="checkbox"/>
Justification	
By	
Distribution/	
Availability Codes	
Dist	Avail and/or Special
A-1	

Contents

1. INTRODUCTION	1
2. THE DEVELOPMENT OF ICING IN LAYER TYPE CLOUDS	3
2.1 Instrumentation	3
2.2 Meteorological Situation	3
2.3 Data Sampling Passes	4
2.4 Cloud Data	9
2.5 Data Analysis	20
2.6 Application of Data to Cloud Formation	22
2.7 Icing Rate	23
3. CASE STUDIES OF OTHER MISSIONS	24
3.1 Flight 80-03, 22-23 January 1980	25
3.2 Flight 80-38, 17-18 December 1980	27
4. ICING DATA FROM GERMANY	29
4.1 Instrumentation	29
4.2 Results	29
5. PROJECT SUMMARY	31
5.1 Recommendations	33
REFERENCES	35
LIST OF ABBREVIATIONS	37

Illustrations

1. Schematic Figure of MC-130E Aircraft, Serial No. 40571	4
2. Radiosonde Sounding, Peoria, Illinois, 12Z, 11 December 1979	5
3. Structure of the Atmosphere Prior to the Arrival of the Cold Front Peoria, Illinois at 12Z, 11 December 1979	5
4. Cold Front Location at 00Z, 12 December 1979	6
5. Location of the Data Passes With Respect to Peoria, Illinois	6
6. Time vs Altitude of Data Passes	7
7. Radiosonde Sounding, Peoria, Illinois, 00Z, 12 December 1979	7
8. ASSP - Measured Droplet Size Distributions for Outside, in the Transition Region and in the Cloud are Shown	9
9. JW-LWC vs Time for Passes No. 1 to No. 3	10
10. Averaged ASSP - Measured Droplet Spectra for the Selected Sections of Pass No. 1, Flight 79-50, 11 December 1979	11
11. Averaged ASSP - Measured Droplet Spectra for Selected Sections of Pass No. 2, Flight 79-50, 11 December 1979	12
12. Averaged ASSP - Measured Droplet Spectra for Selected Section of Pass No. 3, Flight 79-50, 11 December 1979	12
13. Averaged ASSP - Measured Droplet Spectra for Selected Section of Pass No. 3, Zone 1, Flight 79-50, 11 December 1979	14
14. Averaged ASSP - Measured Droplet Spectra for Selected Section of Pass No. 3, Zone 2, Flight 79-50, 11 December 1979	14
15. Averaged ASSP - Measured Droplet Spectra for Selected Section of Pass No. 3, Zone 3, Flight 79-50, 11 December 1979	15
16. Averaged ASSP - Measured Droplet Spectra for Selected Section of Pass No. 3, Zone 4, Flight 79-50, 11 December 1979	15
17. Averaged ASSP - Measured Droplet Spectra for Selected Section of Pass No. 3, Zone 5, Flight 79-50, 11 December 1979	16
18. JW LWC vs Time for Passes No. 5 to No. 7	18
19. Averaged ASSP - Measured Droplet Spectra for Selected Section of Pass No. 5, Flight 79-50, 11 December 1979	18
20. Averaged ASSP - Measured Droplet Spectra for the Selected Section of Pass No. 6, Flight 79-50, 11 December 1979	19
21. Averaged ASSP - Measured Droplet Spectra for the Selected Section of Pass No. 7, Flight 79-50, 11 December 1979	19
22. Averaged ASSP - Measured Droplet Spectra for the Selected Section of Pass No. 4, Flight 79-50, 11 December 1979	20
23. Vertical Profiles of Averaged LWC and Droplet Concentration Spanning Passes No. 1 to No. 7	23
24. Data From PMS 2-D Probes, Recorded During a Passage Through the Frontal Zone near Greensboro, North Carolina on 23 January 1980	24
25. Data From PMS 2-D Probes, Recorded During a Passage Through the Frontal Zone Near Flint, Michigan on 18 December 1980	25

Illustrations

26. Radiosonde Sounding, Greensboro, North Carolina, 00Z, 23 January 1980	26
27. Surface Features, 00Z, 23 January 1980	26
28. Surface Features, 00Z, 18 December 1980	27
29. Radiosonde Sounding, Flint, Michigan, 00Z, 18 December 1980	28
30. Profile of Flight Test No. 47, 22 February 1979	30
31. Averaged ASSP Measured Droplet Spectra for the Maximum Icing Rate in Sections of Pass No. 7	32

Tables

1. Data Measured in Zones of Pass No. 3	16
2. Averaged Data for the Most Intense Regions of Each Cloud Layer	21

Some Microphysical Processes Affecting Aircraft Icing-Final Report

1. INTRODUCTION

In recent years a considerable amount of research on the effects of aircraft icing has been completed. Bragg¹ explored the way ice accumulates on an aircraft surface and how it affects the performance of the aircraft. Hansman and Hollister² and Hansman³ discussed the possibility of using microwaves and electric fields to prevent icing on aircraft. Sayward⁴ told of efforts to reduce the adhesion strength of ice. Reinman, Shaw, and Olsen⁵ described the work being done by the National Aeronautics and Space Administration in the area of the prevention of icing and the removal of ice as it accumulates.

The University of Wyoming and the Federal Aviation Administration have been exploring the microphysical processes involved in the formation of aircraft icing. Politovich⁶ noted that icing rates experienced by the University of Wyoming's King Air aircraft increased with height to match the trends in droplet size and Liquid Water Content (LWC). Politovich⁷ also observed a correlation between droplet diameter and the amount of icing, and states that the size, rather than the number of droplets will determine the rate of icing. Her results also show particle diameters of 10 to 20 μm as being most likely to be present during icing situations. Masters⁸ shows that droplets of this size are quite common in supercooled clouds.

(Received for publication 6 May 1985)

(Due to the large number of references cited above, they will not be listed here. See References, page 35.)

although at a warmer temperature large droplets will predominate. His work is based on data compiled by Jeck.⁹

The Aircraft Icing Probabilities Program of the Air Force Geophysics Laboratory (AFGL) has provided microphysical observations of clouds which caused ice to form on an aircraft. In addition, data from other sources have been examined to see if the microphysical observations made by AFGL compare to those made elsewhere.

The use of an Axially Scattering Spectrometer Probe (ASSP) manufactured by Particle Measuring Systems, Inc., supplemented by 1-D and 2-D cloud and precipitation probes has allowed us to measure particle distributions and obtain shadowgraphs of particle shapes in icing situations. Another technique, exposing oil-covered slides to the atmosphere, was used by the Bundesamt Fur Wehr Technik und Beschaffung (BWB) of the Federal Republic of Germany. They kindly made some of their data available to us, and it is discussed later in this report.

Barnes, Cohen and McLeod¹⁰ described the MC-130E, (flown for AFGL by the 4950th Test Wing, Wright-Patterson AFB, Ohio) which made data-gathering flights into conditions favoring aircraft icing. The AFGL icing flight program consisted of 25 flights, which are listed by Cohen.¹¹ The principal icing detector used was the Rosemount Ice Detector, Model 871FA. Glass and Grantham¹² described the instrument and discussed its response to icing conditions. A similar instrument was used on the BWB flights, although it was not considered by them to be the primary instrument for estimating ice accumulation.

Further findings of the AFGL Icing Program have been reported by Glass¹³ and Cohen.¹⁴ These reports have dealt with the icing detector and its response to supercooled clouds and have compared visual and icing detector observations of icing to forecasts made using rawinsonde information and current forecasting techniques.

This report will look at the droplet spectra of clouds, some of which produced icing, and others which did not. Section 2 examines the microstructure of clouds that led to icing on one of our icing flights. Section 3 examines 2-D shadowgraphs obtained on two flights, one of which produced much less icing than expected and one which produced substantial icing. Section 4 reports on the data AFGL obtained from the BWB in Germany.

(Due to the large number of references cited above, they will not be listed here. See References, page 35.)

2. THE DEVELOPMENT OF ICING IN LAYER TYPE CLOUDS

The extent of aircraft icing is principally a function of the supercooled liquid water content (LWC) of the cloud it penetrates. The amount of LWC encountered is in turn a function of the concentration and size distribution of the supercooled water droplets in the cloud. In order to solve the icing problems for modern aircraft the researcher must completely understand the microphysical processes involved in the development of supercooled clouds. The data presented here will examine the developmental stages of layer type clouds that formed near Peoria, Illinois on 11 December 1979.

2.1 Instrumentation

A list of the cloud physics instrumentation and their location on board the MC-130E aircraft is shown in Figure 1. The main instruments used to measure the meteorological conditions associated with cloud formation and icing are: the Rosemount Total Temperature Probe (No. 6) for obtaining true air temperature, the Johnson-Williams meter (No. 10) for determining LWC from droplets of diameter $\leq 30 \mu\text{m}$; the Particle Measuring System's Axially Scattering Probe (ASSP) (No. 2) for obtaining droplet number concentration, LWC and median volume diameter; and the Rosemount Icing Rate Meter (No. 19). These instruments and the others are described in detail by Glass and Grantham.¹²

2.2 Meteorological Situation

Figure 2 shows the temperature and dew-point profiles from the radiosonde observation on 11 December 1979 at 12Z (GMT) from the Weather Service Office (WSO) Peoria, Illinois. This was approximately 12 hours prior to the passage of the cold front. Two moist layers, were present, one at 850 mb, 93 percent R. H., the other at 650 mb, 60 percent R. H., as depicted in Figure 3. When the cold front arrived, Figure 4, cloud layers were noted to have formed where these moist layers had been. At the surface, the cold front moved through the Peoria area at approximately 1600Z, the wind direction eventually changed from 180° - 190° to 300° - 320° and the temperature dropped from 50°F to 30°F . The latitude-longitude positions and the time vs altitude plot of the seven individual data passes made by the MC-130E aircraft are shown in Figures 5 and 6 respectively. It was not possible for the Mission Director to structure the ascending passes directly over one another. It was his intention to keep the data passes within the same cloud mass. The flight time and location, coincided with the release of the 0000Z, 12 December 1979 radiosonde from Peoria. The skew-T plot of temperature and dew-point from that observation is shown in Figure 7.

MC-130E 40571

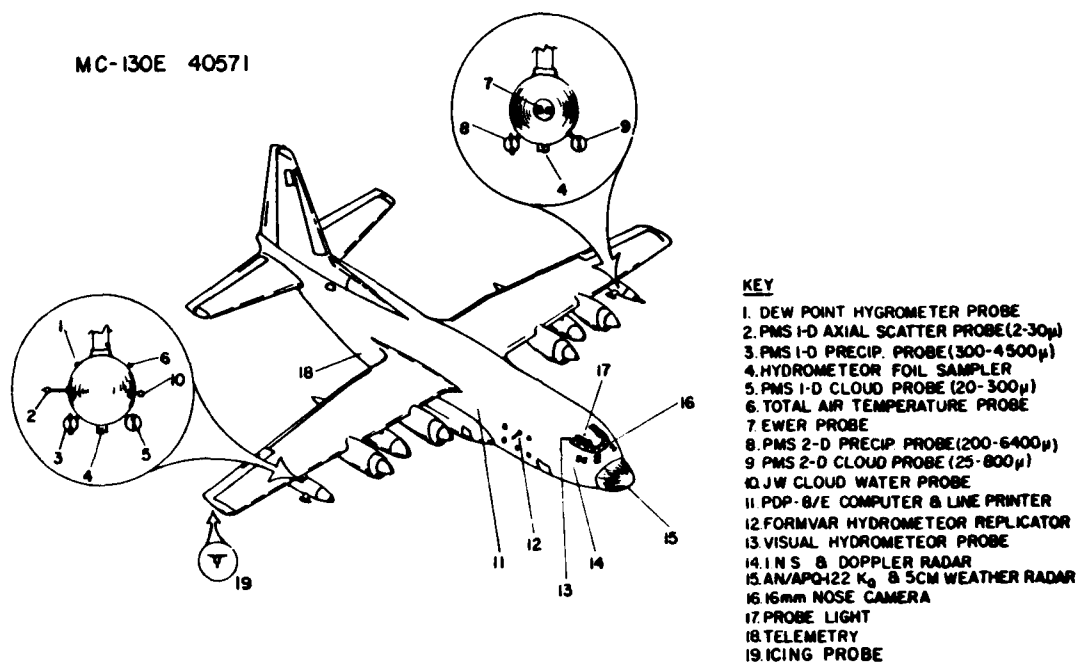


Figure 1. Schematic Figure of MC-130E Aircraft, Serial No. 40571. The cloud physics instrumentation and location on aircraft are shown

2.3 Data Sampling Passes

The 7 passes (Figure 5) flown on 11 December 1979, cover the altitude range of observed cloud conditions. The clouds of interest were structured into two distinct layers; layer No. 1 extended from 1850 m to 3080 m. The top was very close to the 0°C isotherm, so for the most part, the particles in this layer were in the liquid water state. Layer No. 2 extended from 4320 m (base) to 4950 m (top). Layer No. 2 was cold enough to cause icing conditions. The zone between the top of layer No. 1 and the base of layer No. 2 was essentially free of any form of cloud development. However, the PMS Axially Scattering Spectrometer Probe (ASSP) appeared to indicate the presence of aerosols or haze particles in the environmental external to the cloud. These particles were detected in channel No. 1 of the ASSP which had a diameter detection range of 1 μ m to 3 μ m.

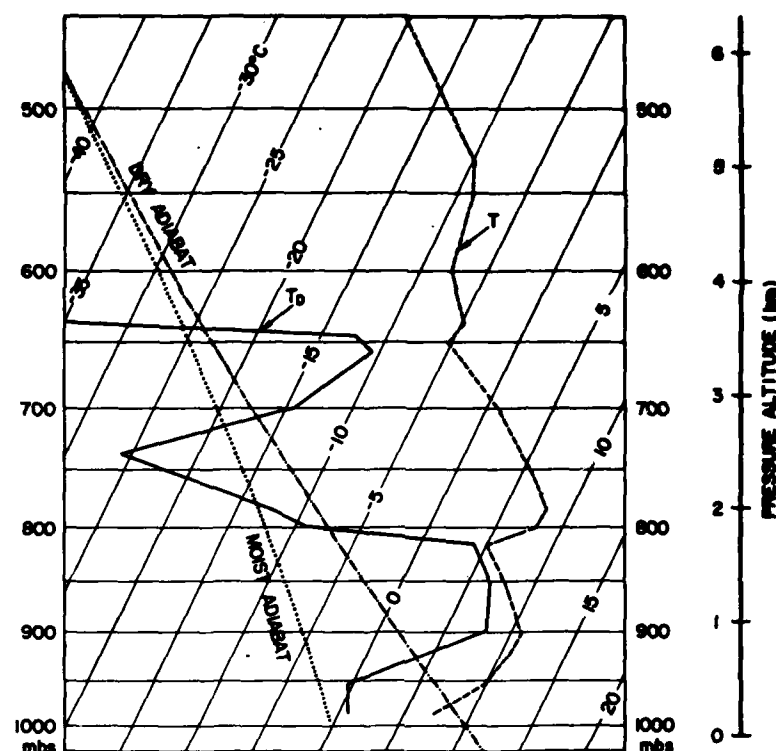


Figure 2. Radiosonde Sounding, Peoria, Illinois, 12Z, 11 December 1979

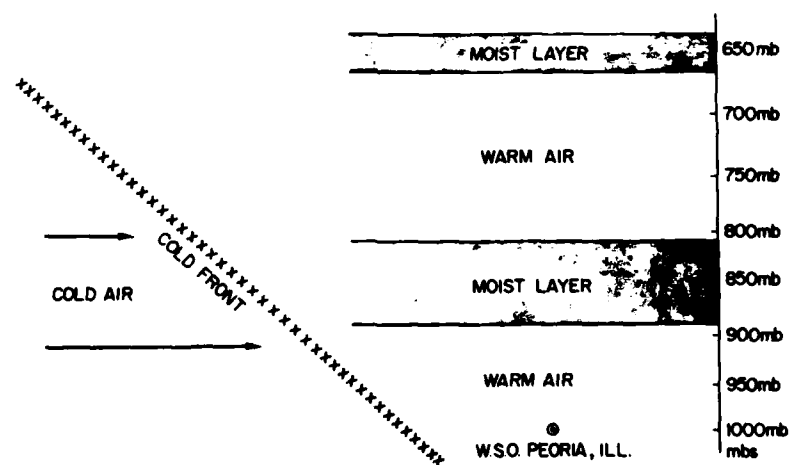


Figure 3. Structure of Atmosphere Prior to the Arrival of the Cold Front, Peoria, Illinois at 12Z, 11 December 1979

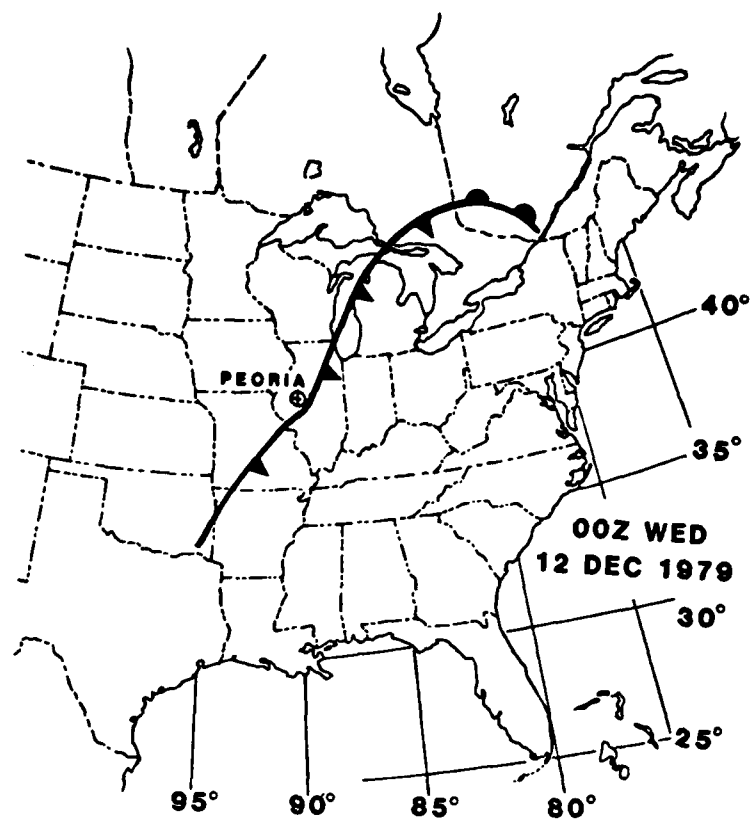


Figure 4. Cold Front Location at 00Z, 12 December 1979

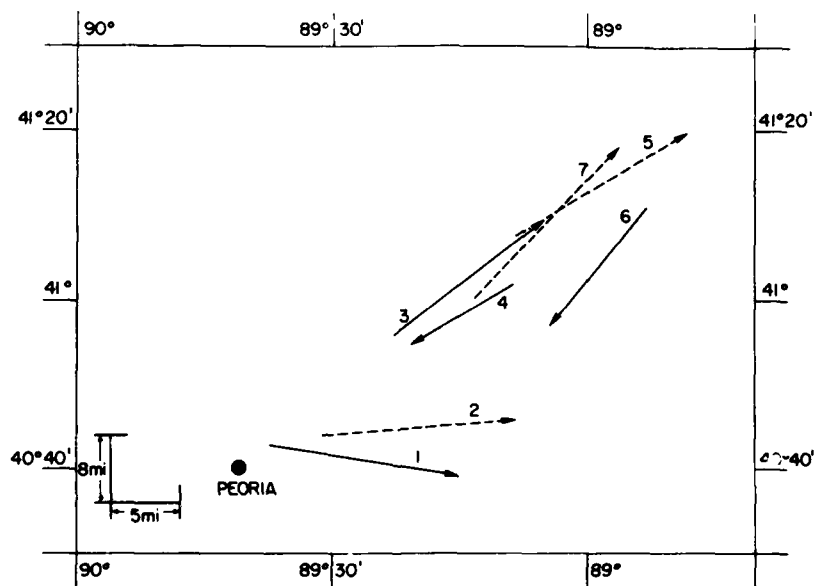


Figure 5. Location of the Data Passes With Respect to Peoria, Illinois

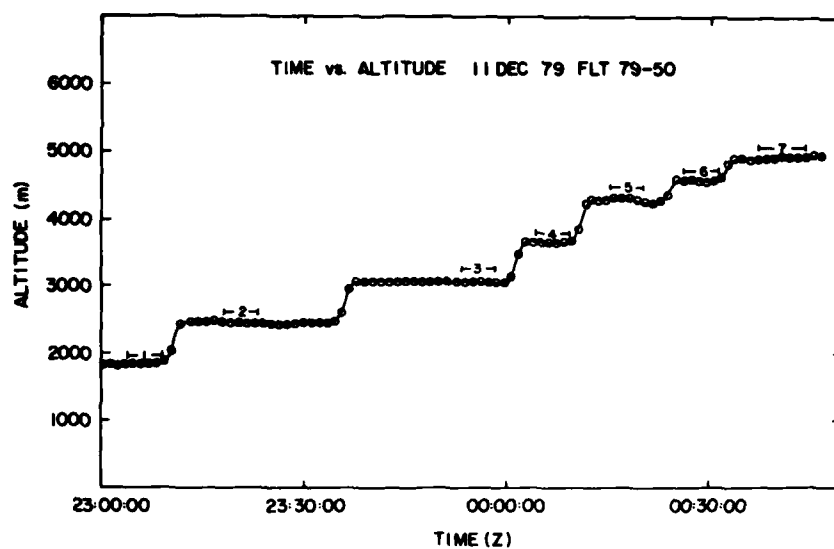


Figure 6. Time vs Altitude Plot of Data Passes

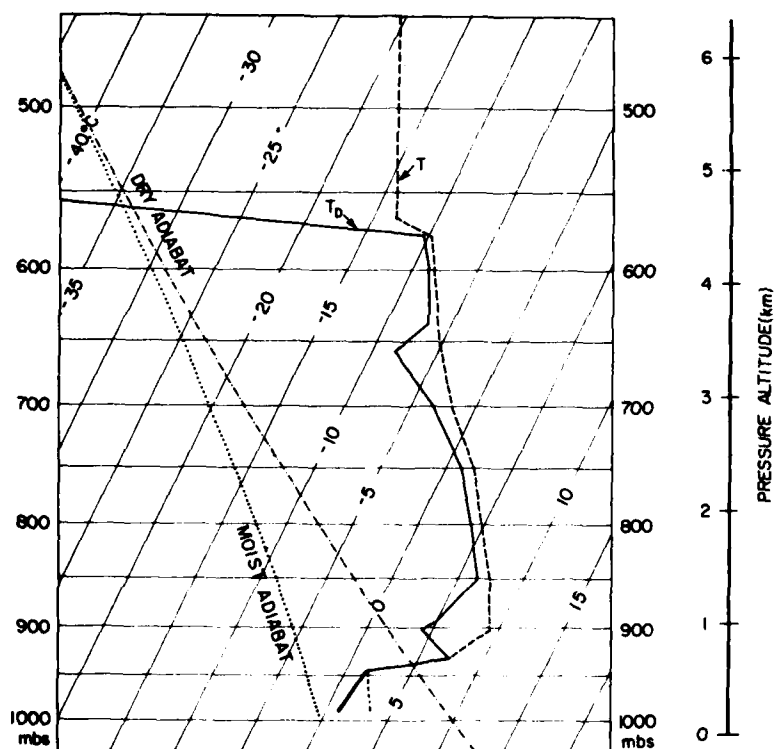


Figure 7. Radiosonde Sounding, Peoria, Illinois, 00Z, 12 December 1979

During the different condensation growth periods encountered, channel No. 1 of the ASSP appeared to respond reasonably with $2.0\text{ }\mu\text{m}$ diameters particle counts. For example, in Figure 8 three droplet size distributions are shown. The first one coded with the symbol 'O', shows the average count of particles in channel No. 1 detected in the clear region outside the cloud. The second distribution, coded with the symbol 'X', shows the sizes of the particles in the transition region at the edge of the cloud. The third, coded with the symbol 'Δ', shows the size distribution of the particles detected a short distance into the cloud. These distributions suggest the initial growth of the cloud water droplet size spectrum from the nuclei size particles of approximately $2.0\text{ }\mu\text{m}$ diameter detected by channel No. 1 of the ASSP. The impact collection efficiency, or aggregation rate, of particles less than $8\text{ }\mu\text{m}$ in diameter is extremely low so that particle growth in this size region is due to condensation alone. If, in this region one assumes that the condensation growth affects the $2.0\text{ }\mu\text{m}$ water particles, then the spectrum produced in the transition region strongly resembles an exponential size distribution (solid line in Figure 8). The decrease in particle counts in channel No. 1 of the ASSP, supports its legitimacy, as the cloud droplet population grows in size and number. This suggests that the concentration of particles with diameters $\leq 2.0\text{ }\mu\text{m}$ are decreasing while the concentration of cloud particles with diameters $> 2.0\text{ }\mu\text{m}$ are increasing. For particle growth by condensation alone, these changes in concentration are consistent with theory. The growth of drop size distributions shown in Figure 8, offers additional evidence that the droplet counts in channel No. 1 are real and not just noise.

Ludwig and Robinson¹⁵ carried out a program of aerosol and cloud droplet measurement in stratus clouds during the summer of 1968 in the hills south of San Francisco. Size distributions were determined with three separate particle size counters measuring particle radii ranging from $0.05\text{ }\mu\text{m}$ to $40.0\text{ }\mu\text{m}$. The size distribution data showed a mode in the submicron range with particle sizes extending up to and beyond the $1.0\text{ }\mu\text{m}$ radius size region. Secondary modes occurred at radii of about 6 to $8\text{ }\mu\text{m}$ in mature clouds. Their observations also show organic material to be present in the nuclei and a nonuniformity in the distribution of sulfur compounds and chlorides over the droplet spectrum. It appears that the activity of the sulfates as droplet nuclei is largely size dependent. The small sulfate particles are inactive and grow little. The larger particles are active and grow to larger droplets, leaving a minimum in the spectrum between the growing droplets and the inactivated particles. In fog studies, at Otis AFB, Kunkel¹⁶ observed that the onset of fog was often preceded by a high concentration of particles of radius $\leq 1.25\text{ }\mu\text{m}$.

15. Ludwig, F. L., and Robinson, E. (1970) Observations of aerosols and droplets in California stratus. *Tellus*, 22:92-105.

16. Kunkel, B. A. (1982) Microphysical Properties of Fog at Otis AFB, AFGL-TR-82-0026, AD A119928.

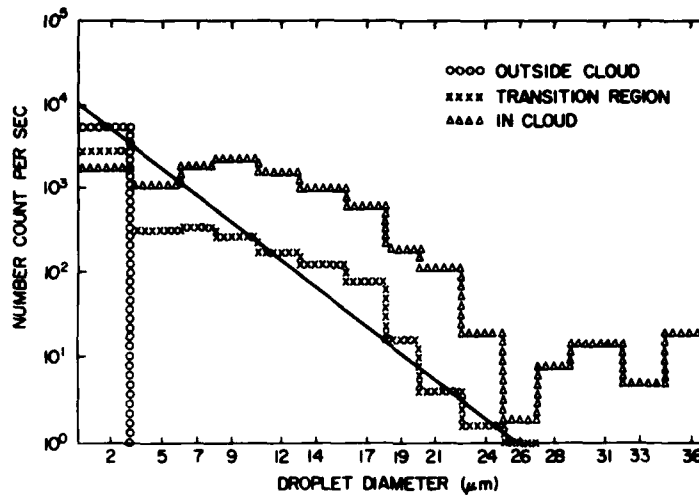


Figure 8. ASSP - Measured Droplet Size Distributions for Outside, in the Transition Region and in the Cloud are Shown. ASSP channel numbers are indicated along the abscissa

2.4 Cloud Data

The data collection passes in the cloud were conducted at constant altitude and heading and all were 3 to 5 min long. Although the values of the measured parameters varied considerably within individual passes, there were regions which showed noticeable increases in LWC values. The LWC values* presented herein have been corrected by the bulk bias removal method suggested by Glass and Grantham.¹² It is the authors opinion that the JW is over responding to the small wet particles with diameters $\leq 2.0 \mu\text{m}$. As the concentration of these particles decrease with increasing altitude and decreasing temperature and humidity, the zero calibration appears to return to its normal correct reading. These types of discrepancy high-light the need for additional research in the LWC measurement area, directed toward some convenient means of calibrating these instruments to known standards as recommended by Ide and Richter¹⁷ and Baumgardner.¹⁸

*The reviewers of this manuscript noted that the uncorrected JW LWC values were too high: (1) outside the cloud and (2) when compared to the LWC values generated by the ASSP.

17. Ide, R. F., and Richer, G. P. (1984) Comparison of Icing Cloud Instruments for 1982-1983 Icing Season Flight Program. NASA-TM-83569; E-1950; NAS 1 15:83569; USAAVSCOM-TR-84-C-1, 19 pp.

18. Baumgardner, D. (1983) An analysis and comparison of five water droplet measuring instruments. J. Appl. Meteor. 22:891-910.

Assuming that the larger cloud particles grow in cell type developments, regions showing the highest values of measured parameters were chosen in the hope that these measured parameters would better characterize the growth region. Figure 9 shows the JW LWC values produced in selected sections of the three passes through layer No. 1. Pass No. 1, at the base of the cloud, is coded by the symbol 'X'. Pass No. 2, in the midsection of the cloud, is coded by the symbol 'O', and Pass No. 3, at the top of the layer, is coded by the symbol 'Δ'. The tick marks, labeled 'start' and 'end' on each of the data plots, show the regions over which the LWC values and the other measured parameters have been averaged. These average values are shown in Figures 10, 11, and 12, for Passes No. 1, No. 2 and No. 3 respectively. A definite growth of droplet size with altitude is evident. The JW liquid water content (LWC) values increase from 0.19 g/m^3 to 0.48 g/m^3 to 0.73 g/m^3 in ascending order. The peak in the droplet size distribution as measured by the ASSP increases from $5 \text{ }\mu\text{m}$ to $7 \text{ }\mu\text{m}$ to $9 \text{ }\mu\text{m}$ in a similar manner.

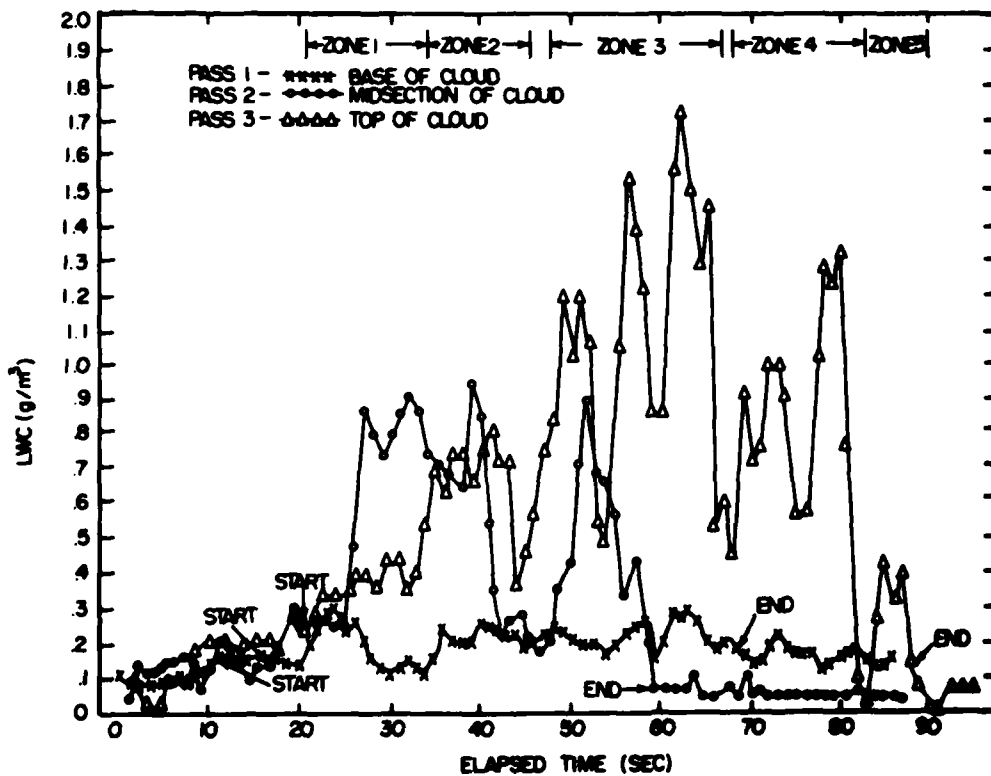


Figure 9. JW-LWC vs Time for Passes No. 1 to No. 3. Selected sections for each are indicated by 'start' and 'stop'

These measurements clearly indicate a growth pattern with height above cloud base. Similar growth patterns by condensation have been presented by Mason and Chien¹⁹ and by Lee, Hanel and Pruppacher²⁰ and are associated with uplifting.

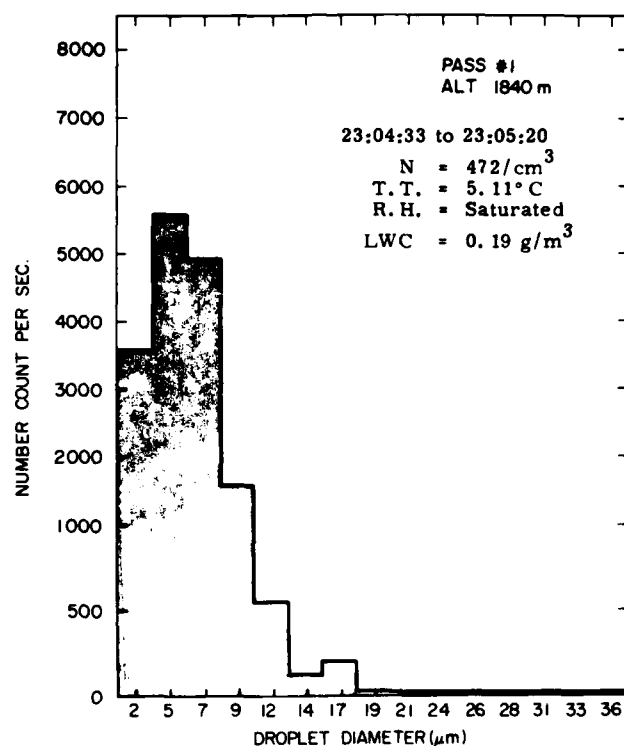


Figure 10. Averaged ASSP - Measured Droplet Spectra for the Selected Sections of Pass No. 9, Flight 79-50, 11 December 1979. T.T. is true temperature and LWC values are from the JW probe

19. Mason, B.J., and Chien, C.W. (1962) Cloud-droplet growth by condensation in cumulus, Quart. J.R. Met. Soc. 88:136.
20. Lee, I.Y., Hanel, G., and Pruppacher, H.R. (1980) A numerical determination of the evolution of cloud drop spectra due to condensation on natural aerosol particles, J. Atmos. Sci. 37(No. 8):1839.

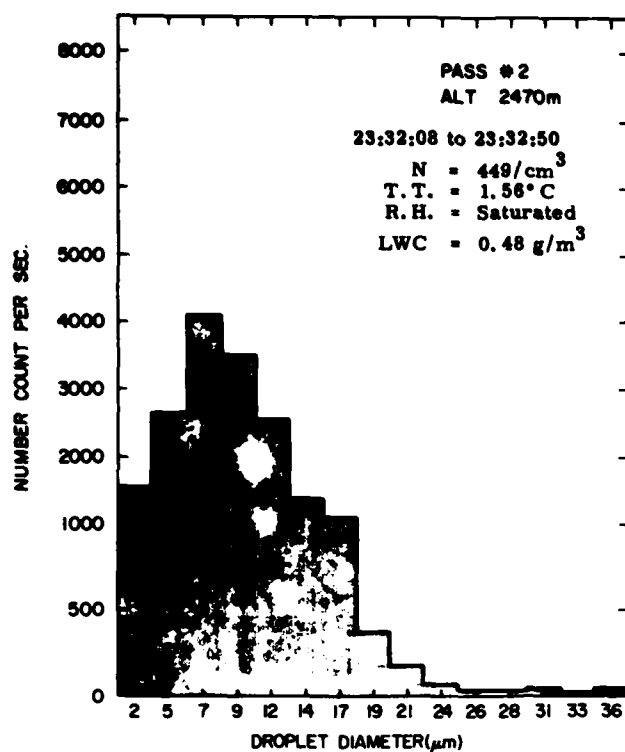


Figure 11. Averaged ASSP - Measured Droplet Spectra for Selected Sections of Pass No. 2, Flight 79-50, 11 December 1979

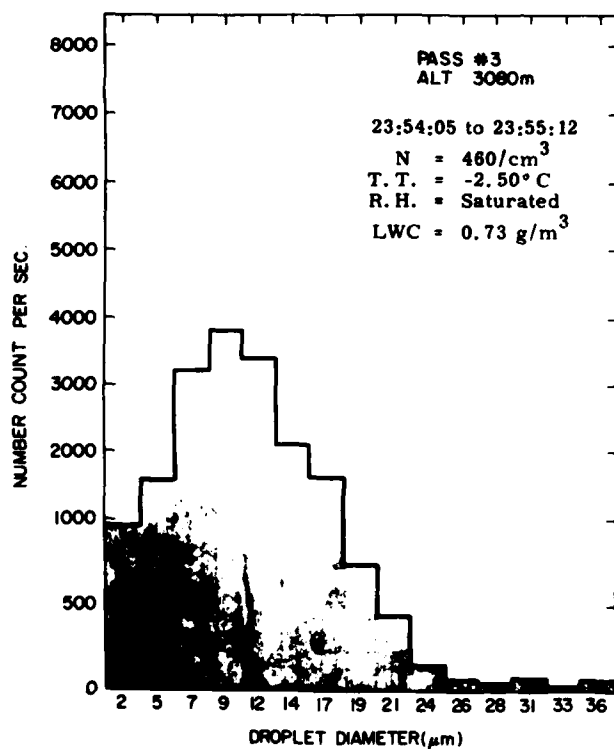


Figure 12. Averaged ASSP - Measured Droplet Spectra for Selected Section of Pass No. 3, Flight 79-50, 11 December 1979

Based on the amplitude variations of LWC values plotted in Figure 9, we have divided Pass No. 3 into five sections, hereafter referred to as zones. The data on cumulus cloud cell development shown in Figures 13 to 17 were recorded during Pass No. 3 at the top of layer No. 1 over the 23:54:05 to 23:55:12 time span. The data values shown in Figures 13 to 17 are the result of averaging over selected time spans. A more detailed look at the LWC values plotted in Figure 9 shows that the LWC values for Pass No. 3 are really made up of five zones, the first three of which increase in magnitude with elapsed time. Zone 1 having a time span from 23:54:04 to 23:54:17 is shown in Figure 13. The averaged data for Zone 1 shows values of $LWC = 0.33 \text{ g/m}^3$ and a mode diameter of $7.0 \text{ }\mu\text{m}$. Zone 2 having a time span from 23:54:19 to 23:54:27 is shown in Figure 14. The averaged data for Zone 2 indicates a LWC of 0.71 g/m^3 and a mode diameter of $9.0 \text{ }\mu\text{m}$. Zone 3 having a time span from 23:54:32 to 23:54:49 is shown in Figure 15. This zone represents the core of the cell, with the largest values of $LWC = 1.16 \text{ g/m}^3$ and mode diameter $= 12.0 \text{ }\mu\text{m}$. On the lee side of the cumulus cell, two zones of LWC values are indicated in Figures 16 and 17. These decrease in magnitude with elapsed time. Zone 4 having a time span from 23:54:53 to 23:55:06 is shown in Figure 16. The averaged data for Zone 4 shows a LWC value of 0.90 g/m^3 and a mode diameter of $12 \text{ }\mu\text{m}$. Zone 5 covering the time span from 23:55:09 to 23:55:12 is shown in Figure 17. The averaged data for Zone 5 shows a LWC value of 0.36 g/m^3 and a mode diameter of $9.0 \text{ }\mu\text{m}$. Although the data from the five zones were recorded at the same altitude and in the dome of the same developing cumulus cell, some of the measured parameters showed significant zone to zone differences in values. Figure 15, representing Zone 3, having the largest values of LWC and mode diameter, appears to be the core of the developing cell. We now look at the 00Z, 12 December 1979, Peoria, Illinois, radiosonde wind measurements. At 3080 m above ground level, the wind speed was 50 knots and the wind direction was 235° . During Pass No. 3, the aircraft magnetic heading varied between 34.52° and 46.95° . It therefore was travelling in approximately the same direction as the wind when it traversed the dome of the cell. The midpoint of Zone 3 was approximately in the middle of Pass No. 3. Zones 1 and 2 were positioned upwind of Zone 3 and Zones 4 and 5 were positioned downwind. Zones 1 and 5 and Zones 2 and 4 were approximately equidistant from the center of Zone 3. The averaged data measured in each of the five zones of Pass No. 3 are shown in Table 1.

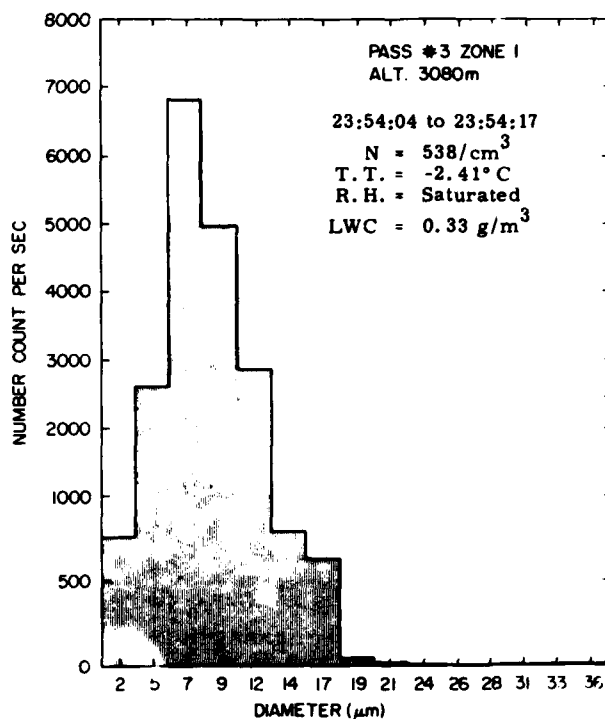


Figure 13. Averaged ASSP -
Measured Droplet Spectra
for Selected Section of
Pass No. 3, Zone 1,
Flight 79-50, 11 December 1979

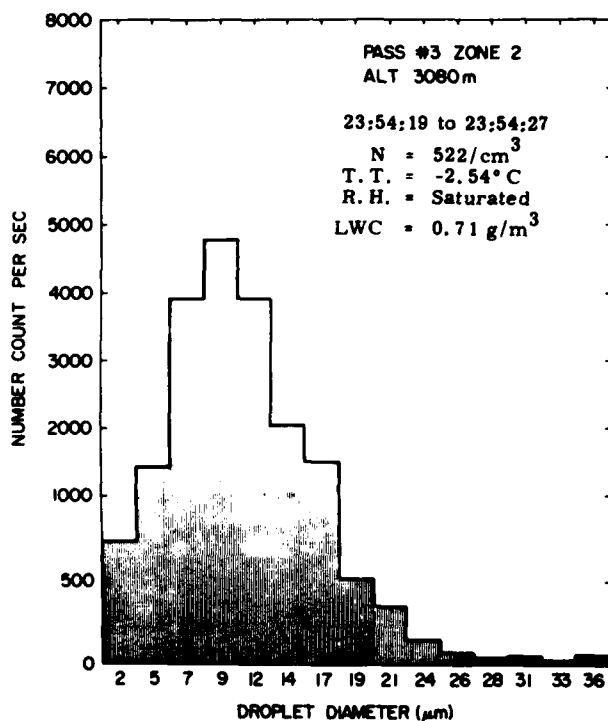


Figure 14. Averaged ASSP -
Measured Droplet Spectra
for Selected Section of
Pass No. 3, Zone 2,
Flight 79-50, 11 December 1979

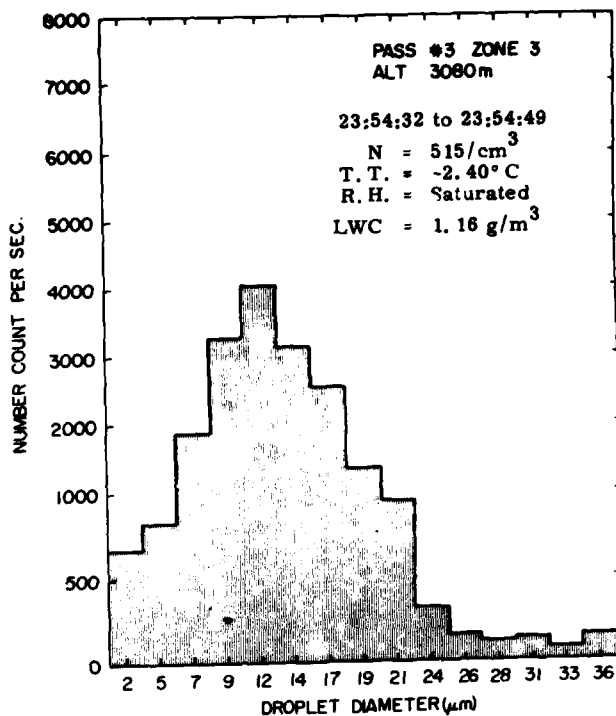


Figure 15. Averaged ASSP - Measured Droplet Spectra for Selected Section of Pass No. 3, Zone 3, Flight 79-50, 11 December 1979

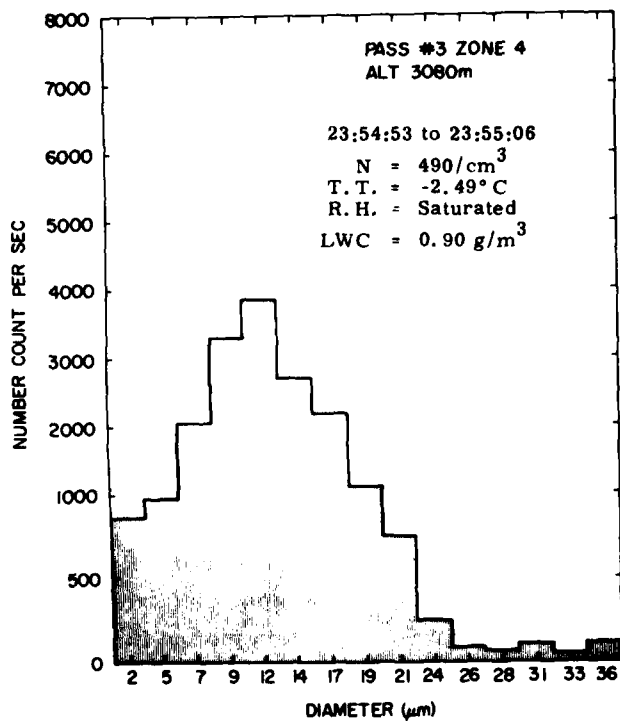


Figure 16. Averaged ASSP - Measured Droplet Spectra for Selected Section of Pass No. 3, Zone 4, Flight 79-50, 11 December 1979

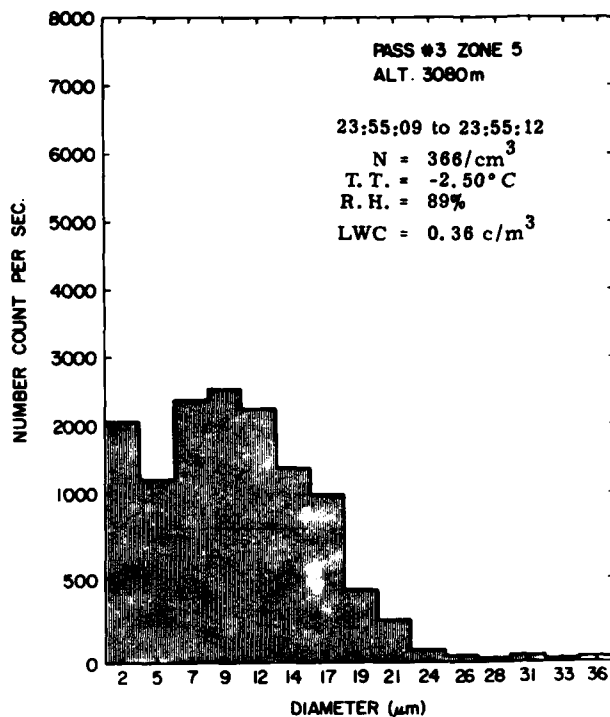


Figure 17. Averaged ASSP - Measured Droplet Spectra for Selected Section of Pass No. 3, Zone 5, Flight 79-50, 11 December 1979

Table 1. Data Measured in Zones of Pass No. 3

Data	Zone 1	Zone 2	Zone 3	Zone 4	Zone 5	Dimensions
Particle Concentration	538	522	515	490	366	No. /cm ³
Liquid Water Concentration (LWC)	0.33	0.71	1.16	0.90	0.36	g/m ³
True Temperature	-2.57	-2.54	-2.40	-2.49	-2.50	°C
Relative Humidity	Saturated		Saturated		90	%
Mode Diameter	7.0	7.0	12.0	12.0	9.0	μm

The LWC and mode diameter values tend to decrease in amplitude as the distance increases from the center. Although Zone 4 shows the same mode diameter value of 12 μm as Zone 3, a close look at the particle size distribution plotted in Figure 16 shows the distribution is skewed toward a value lower than 12 μm. The LWC and mode diameter values are larger in Zones 4 and 5 than the corresponding values

in Zones 2 and 1. The number of particles counted per second does not decrease between Zone 3 and Zone 1. This suggests the absence of the coalescence process in the upwind peripheral zone. The LWC and mode diameter values decrease away from the center suggesting that evaporation may be taking place. On the peripheral edge of a cloud, evaporation is caused by the mixing of the cloud mass with the surrounding drier air. The particle size distribution of Figure 13 shows the results of this evaporation process on particles having diameters $\geq 9.0 \mu\text{m}$. A large number of these particles have apparently been reduced in size producing a large count in the $7.0 \mu\text{m}$ diameter channel of Figure 13. Both Zone 1 and Zone 5 are edge regions of the cloud; Zone 1 being the windward peripheral formation edge and Zone 5 the leeward peripheral dissipation edge. The mixing mechanisms responsible for their individual drop size distributions are quite different.

The Mission Director observed slight icing on the snow stick during portions of Pass No. 3. The Rosemount Ice Detector did not respond to these light icing conditions. The Mission Director also noted during Pass No. 3 when the aircraft emerged in clear areas that clouds were visible above and below the aircraft, thus indicating the structured nature of the cloud system.

Cloud layer No. 2 appears to have developed in the same manner as cloud layer No. 1. Figure 18 shows the JW LWC values recorded in selected sections of layer No. 2. These sections at the base, midsection and top of cloud layer No. 2 were selected in the same way as the selections made in cloud layer No. 1, Figure 9. Individual distributions are shown in Figures 19, 20, and 21. The tick marks for the three passes labeled 'start' and 'end' on each of the waveforms show the section of data used to generate an average for the parameters sampled. The droplet size distribution generated by the ASSP for Pass No. 7 at the cloud top is shown in Figure 21. An averaged droplet size distribution over the selected region for Pass No. 6, in the middle of cloud layer No. 2 is shown in Figure 20. The average droplet size distribution over the selected region in Pass No. 5, the base of the cloud, is shown in Figure 19. This particle size distribution suggests that this pass was made at the edge or transition region of the cloud, as also depicted in Figure 8. Again, we note that the mode diameter and LWC values increase as a function of height above cloud base. In fact, cloud layer No. 2 appears to be a reduced version of cloud layer No. 1 in this respect. Unlike cloud layer No. 1, cloud layer No. 2 at an altitude of 4600 m was in an icing environment with temperatures $< 0.^\circ\text{C}$.

Pass No. 4, at an altitude of 3670 m, was made in a clear region between cloud layer No. 1 and cloud layer No. 2. The particle size distribution for this pass is shown in Figure 22 where only the small particles of $2 \mu\text{m}$ diameter are evident.

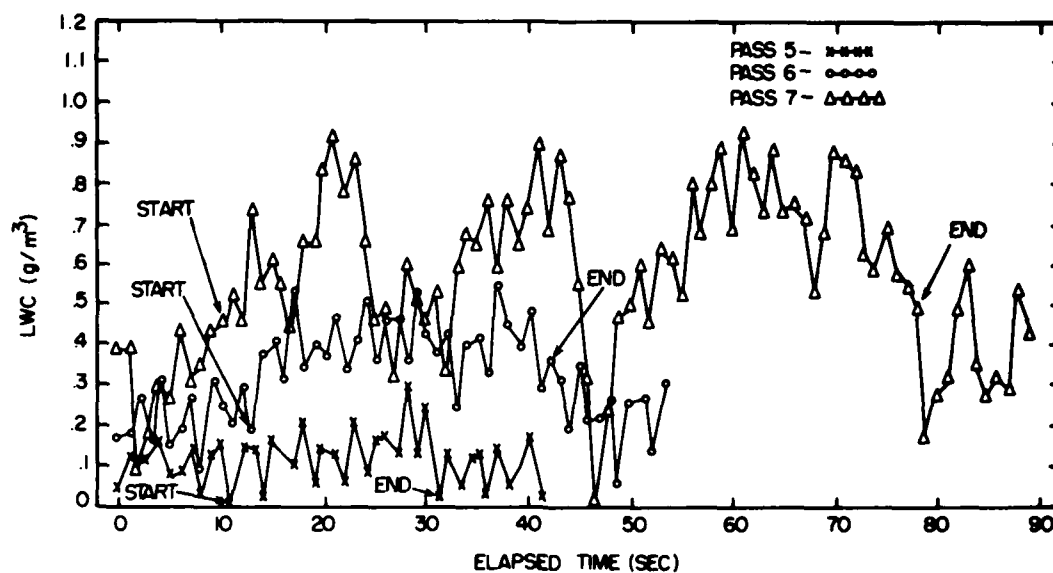


Figure 18. JW LWC vs Time for Passes No. 5 to No. 7. Selected sections are indicated by 'start' and 'stop' for each pass

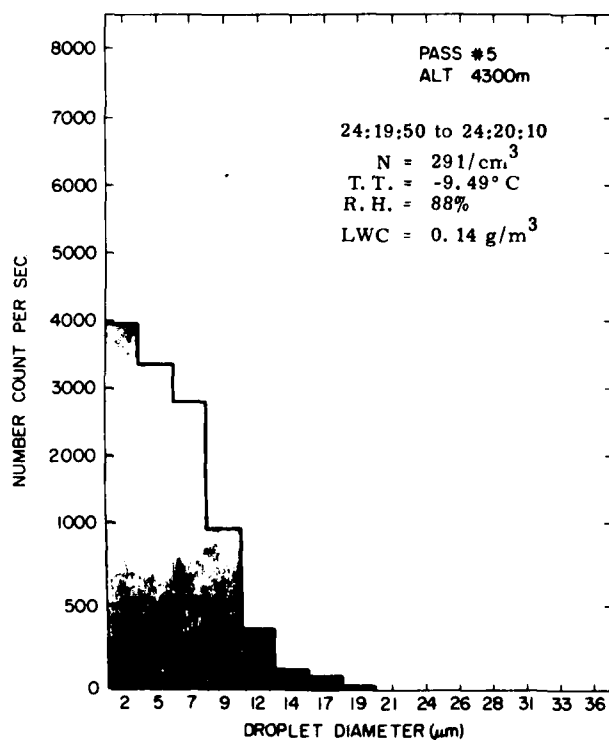


Figure 19. Averaged ASSP - Measured Droplet Spectra for Selected Section of Pass No. 5, Flight 79-50, 11 December 1979

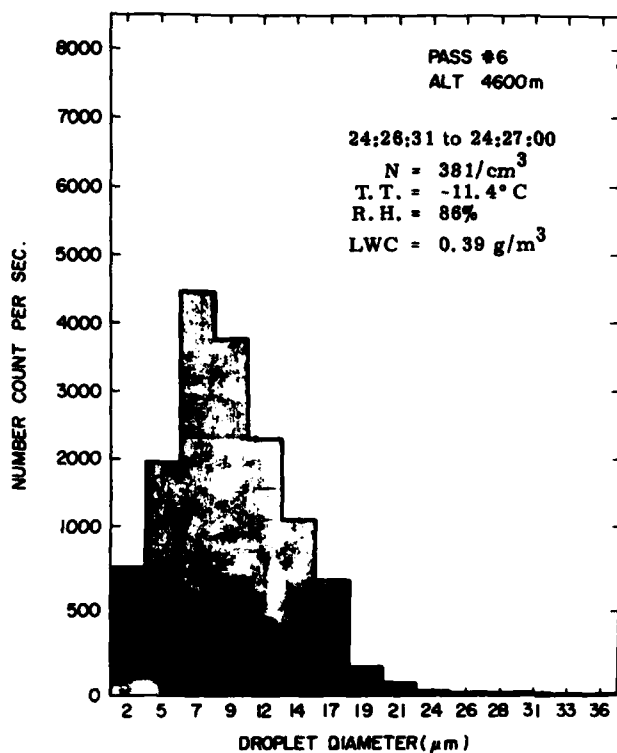


Figure 20. Averaged ASSP - Measured Droplet Spectra for the Selected Section of Pass No. 6, Flight 79-50, 11 December 1979

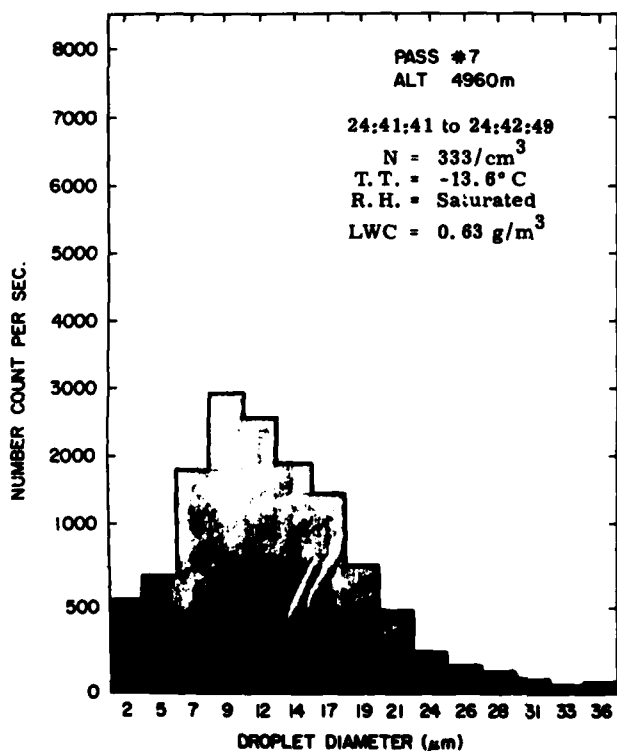


Figure 21. Averaged ASSP - Measured Droplet Spectra for the Selected Section of Pass No. 7, Flight 79-50, 11 December 1979

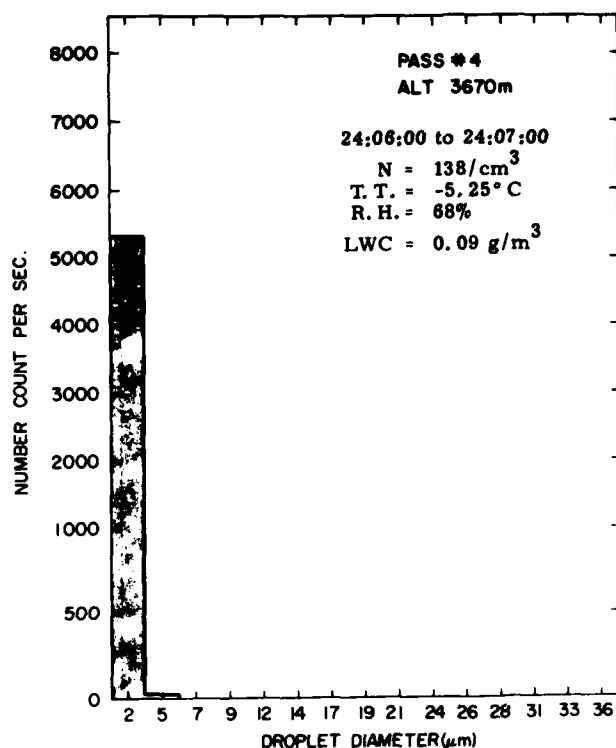


Figure 22. Averaged ASSP - Measured Droplet Spectra for the Selected Section of Pass No. 4, Flight 79-50, 11 December 1979

2.5 Data Analysis

Summary information with the averaged data for the most intense regions of the cloud layers is shown in Table 2. Cloud layer No. 1 shows larger values of cloud depth (ΔH), liquid water content (LWC), and droplet concentration. A comparison of the measurement values produced in cloud layer No. 2, shows that the LWC values increase from 0.39 g/m³ to 0.63 g/m³ in going from Pass No. 6 to Pass No. 7, while the droplet concentration values decrease from 381 particles/cm³ to 333 particles/cm³. This, coupled with a noticeable increase in the number of drops shown in the large diameter tail section of the droplet distribution, Figure 21, suggests the presence of the coalescence process in Pass No. 7. The same type of measurements in cloud layer No. 1 show that the LWC values increase from 0.48 g/m³ to 0.73 g/m³ in going from Pass No. 2 to Pass No. 3, but droplet concentration values increase from 441 particles/cm³ to 462 particles/cm³. The particle size distribution shown in Figure 19 for Pass No. 5 of cloud layer No. 2, strongly resembles an exponential distribution. This type of distribution, together with the low particle concentration of 291 particles/cm³, suggests that this pass was made in the transition zone at the edge of the cloud base. As it turns out, the LWC, mode diameter and droplet concentration values measured in Pass No. 5 were much less than the corresponding measurements in Pass No. 1.

Table 2. Averaged Data for the Most Intense Regions of Each Cloud Layer

Cloud Layer No.	Altitude H to Cloud Base meters	Depth ΔH Meters	LWC g/m ³ at Cloud Top	Droplet (n) per cm ³ Concentrations at Cloud Top	True Temp. °C at Cloud Top	Maximum Mode Diameter at Top of Cloud
Cloud Layer No. 1	1840	1240	0.73 g/m ³	462/cm ³	-2.5°C	9.0 μm
Cloud Layer No. 2	4300	660	0.63 g/m ³	333/cm ³	-13.8°C	9.0 μm
						Zone 3 = 12.0 μm

Consider now the midsections of the two cloud layers, Pass No. 2 and Pass No. 6. We see in Figures 11 and 20 that the value of mode diameter generated in both layers was $7.0\ \mu\text{m}$. It appears that both droplet populations in the midsection of both layers experienced very similar supersaturation environments to produce mode diameter values of $7.0\ \mu\text{m}$. In like manner, the top sections of both clouds, Pass No. 3 and Pass No. 7, depicted in Figures 12 and 21, show that the averaged value of mode diameter generated in both layers was $9.0\ \mu\text{m}$. Again, it appears that both layer tops experienced similar supersaturation environments to produce mode diameter values of $9.0\ \mu\text{m}$.

Returning now to the LWC values measured throughout cloud layers No. 1 and No. 2, we notice that the LWC values measured at all levels in cloud layer No. 1 were consistently larger than the corresponding LWC values measured in cloud layer No. 2. Consider the particle concentrations, for droplet diameters $\geq 2.0\ \mu\text{m}$, measured in both layers. Again, we note that the droplet concentrations measured at all levels in layer No. 1 are consistently larger than the corresponding droplet concentrations measured in layer No. 2. It seems apparent that the LWC values measured in both layers are directly related to the corresponding droplet concentration values measured during the same pass.

2.6 Application of Data to Cloud Formation

As noted previously, the PMS Axially Scattering Spectrometer Probe (ASSP) recorded the presence of aerosols in the environment, external to the cloud formation. These particles were detected in channel No. 1 of the ASSP, which has a diameter detection range of $1\ \mu\text{m}$ to $3\ \mu\text{m}$. It appears that these haze type particles were more numerous in the region corresponding to layer No. 1 prior to cloud development. Measurements taken in a region external to cloud layer No. 1, at an altitude corresponding to that of Pass No. 1, showed that the detected particles in channel 1 had an average concentration of $191\ \text{particles}/\text{cm}^3$. Similar measurements taken in a region external to cloud layer No. 2, at an altitude corresponding to that of Pass No. 5, showed that the detected particles with $2.0\ \mu\text{m}$ diameters had an average concentration of $149\ \text{particles}/\text{cm}^3$. In other words, the precloud area of layer No. 1 had 28 percent more particles than the precloud area of layer No. 2. This excess of available particles is correlated with the LWC and particle concentration measured in layer No. 1 as shown in Figure 23.

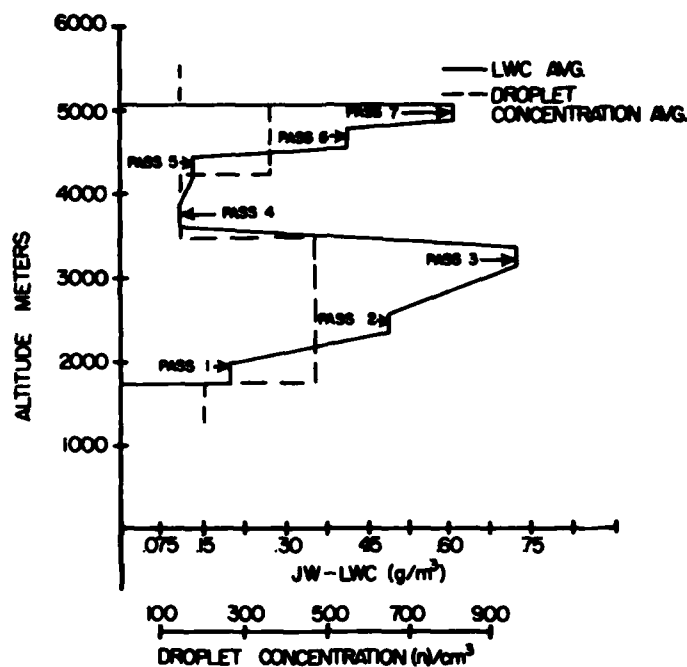


Figure 23. Vertical Profiles of Averaged LWC and Droplet Concentration Scanning Passes No. 1 to No. 7

2.7 Icing Rate

Although cloud layer No. 1 produced relatively high values of liquid water content, it essentially remained above freezing hence no supercooled water droplets were present. The Rosemount Ice Detector did not show any indication of icing during the first three passes. As noted previously, Pass No. 5 in layer No. 2 was positioned on the lower edge of that cloud layer and produce JW liquid water values $\leq 0.14 \text{ gm}^{-3}$, and resulted in a minimal response from the Rosemount Ice Detector. The comments of the Mission Director best describes the icing encountered during Pass No. 5, that is, in and out of clouds, light rime icing in cloud."

During Pass No. 6, the icing was classified as light to moderate and the ice detector, in the core region, on average, took ≈ 22 sec to complete its sensing cycle, corresponding to an icing rate of 1.39 mm/min. In Pass No. 7, where the highest JW liquid water values were recorded ($\text{LWC} = 0.63 \text{ gm}^{-3}$) in the core region, the icing was classified as moderate to heavy and the Rosemount Icing Detector, on average took ≈ 14 sec to complete its sensing cycle, corresponding to an icing rate of 2.18 mm/min.

3. CASE STUDIES OF OTHER MISSIONS

Two other flights have been singled out for examination of 2-D and synoptic data. Using standard synoptic techniques, icing was forecast for both flights. They present a contrast, however, as in one case we expected considerably more icing than was observed while in the other the aircraft encountered if anything, more icing than was expected. We will look at the synoptic situations for these flights, and the crystal types observed by the PMS 2-D probes (Figures 24 and 25).

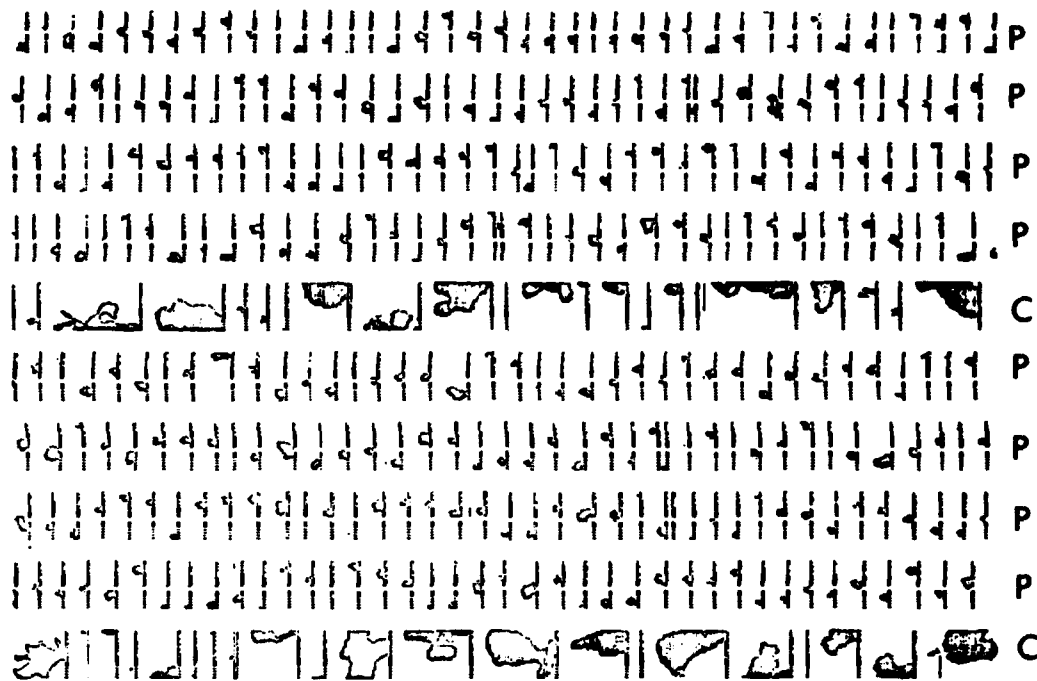


Figure 24. Data From PMS 2-D Probes, Recorded During a Passage Through the Frontal Zone Near Greensboro, North Carolina on 23 January 1980. Lines marked 'P' are images from the 2D-P probe, having a resolution of 200 μm and a vertical image dimension of 6400 μm . Lines marked 'C' are images from the 2D-C probe, having a resolution of 25 μm and a vertical image dimension of 800 μm .

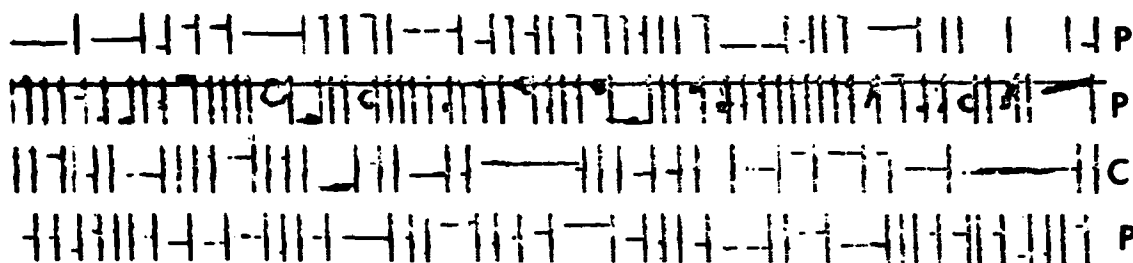


Figure 25. Data From PMS 2-D Probes, Recorded During a Passage Through the Frontal Zone Near Flint, Michigan on 18 December 1980. Line markings and calibration are the same as in Figure 26

Flight 80-03, 22-23 January 1980

On the evening of 22 January 1980, the MC-130 flew an icing mission near Greensboro, North Carolina. As Figure 26 shows, the atmosphere from the cloud base to the 500-mb level was moist, there was a front in the area, and a layer from about 700 mb (3.0 km) to 500 mb (5.0 km) appeared to have great potential for icing. Cohen¹¹ shows that two forecast techniques were used to predict the potential for icing, the Skew-T (SKT) and the Air Force Global Weather Central (AFGWC) method. For Pass No. 1 of Flight 80-03 at an altitude of 4.5 km and a temperature of -9.3°C , the SKT method forecast heavy rime while the AFGWC method forecast moderate rime. In fact, only occasional light icing was observed during the flight. For example, the Pass No. 1 visual observation (VIS) indicated no icing and the average number of cycles of the Rosemount Icing Detector (ICD) was zero.

Figure 27 shows the surface features at the time of the flight. A low pressure area in northern Georgia provided a supply of warm, moist air. The warm front which appears at the surface south of Greensboro, is evident in Figure 26 at 850 mb. Thus, the flight took place in a moist, unstable frontal zone.

This system produced continuous steady rain throughout the frontal zone. As shown in Figure 24, there were many large particles in the area. Our observation showed that most remained in solid form until passing through the freezing level, after which they melted directly into drops. Evidently, most of the particles above the freezing level were in solid form while all of the hydrometeors below the melting level were in liquid form. The drop diameters generally were 400 μm or greater; about 10 or more times the droplet size most frequently associated with aircraft icing. The occasional light icing experienced during this flight was probably the result of the small number of supercooled water droplets available.

One can also note that although the temperature-dew point spread was less than 2°C throughout the temperature range at which icing was likely (-3°C to -16°C), the atmosphere was not saturated.

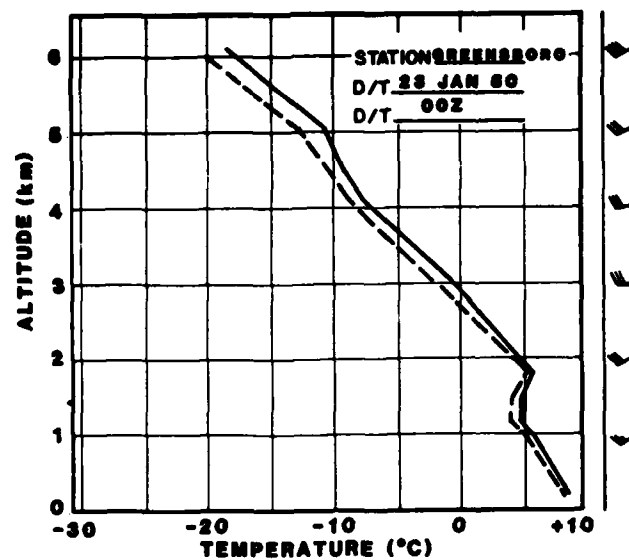


Figure 26. Radiosonde Sounding, Greensboro, North Carolina, 00Z, 23 January 1980

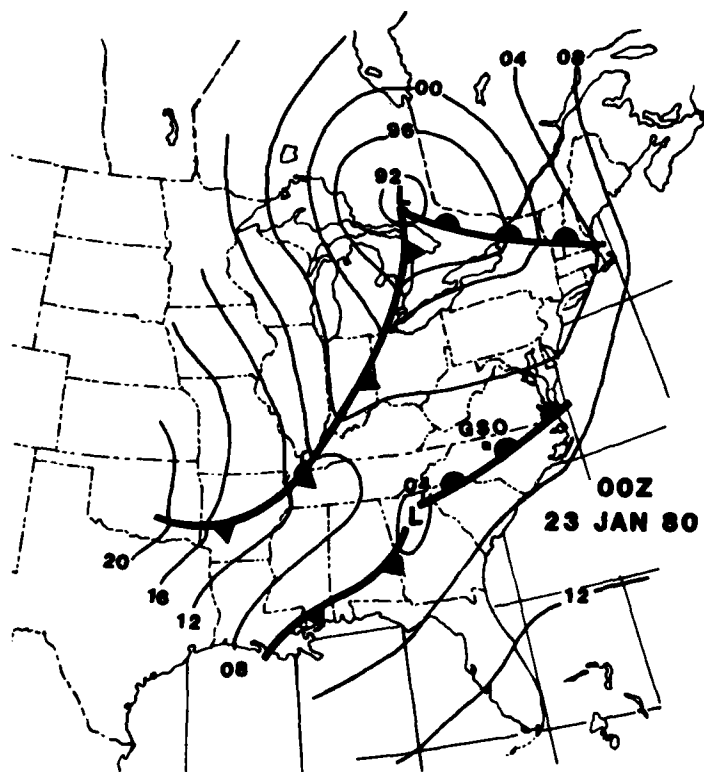


Figure 27. Surface Features, 00Z, 23 January 1980

3.2 Flight 80-38, 17-18 December 1980

This mission flown on the evening of 17 December 1980, sampled clouds near Flint, Michigan. As shown in Figure 28, a warm front was approaching Flint. The surface temperature rose during the evening hours from -4°C at 2200Z (1700 Eastern Standard Time) to $=1^{\circ}\text{C}$ at 0300Z (2200 Eastern Standard Time), as warm air penetrated aloft. The front can be seen in Figure 29 as a strong inversion just above the surface at 1.5 km (850 mb).

Some mixed rain and snow was falling in advance of the front, and occasional rain was reported in the warm sector, but a large precipitation shield, as was present in the previous case, was not evident in this system. Flint reported snow-showers at 2200 and 2300Z. At 00Z, Flint reported 10 miles visibility with no precipitation.

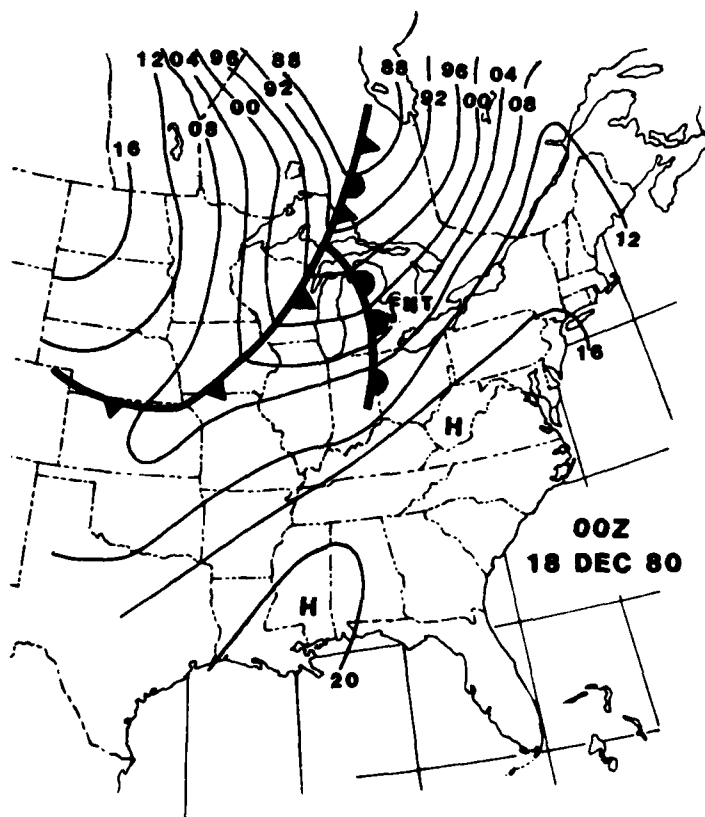


Figure 28. Surface Features, 00Z, 18 December 1980

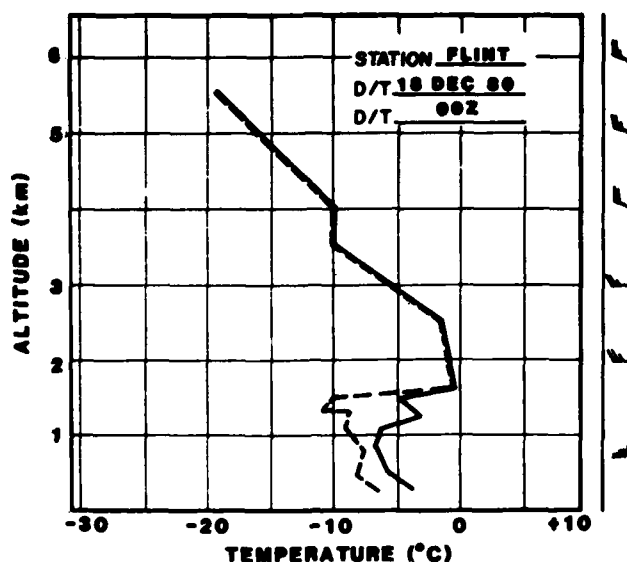


Figure 29. Radiosonde Sounding, Flint, Michigan
00Z, 18 December 1980

Cloud sampling in the area began at 2320Z and ended at 0020Z. Of the eight passes flown, icing was reported on six of them. On two of the passes, the observer reported moderate icing. In Pass No. 7, the icing detector registered 0.99 cycles per nautical mile; equivalent to an icing rate of 2.2 mm/min. This was the most rapid accumulation of ice observed during any of the icing flights. This pass began at 0002Z; thus no precipitation was observed falling at the ground while the aircraft was encountering this intense icing activity.

In comparing the two flights, the microphysical differences are more striking than the synoptic differences. In both cases, the icing occurred in advance of a warm front with strong southerly flow in the mid-troposphere. Both flights examined the altitudes which surrounded the melting layer. In the Greensboro storm there were a substantial number of large, but uniformly sized particles. The Flint storm, in contrast, had a wider variety of particle size and shapes. The Greensboro storm produced heavy precipitation, but little icing, while the Flint storm provided much icing but only spotty precipitation.

4. ICING DATA FROM GERMANY

An aircraft icing program was conducted by the German Flight Test Facility at Manching, Federal Republic of Germany (FRG). This office is part of the Federal Office of Military Technology and Procurement of the FRG (Bundesamt für Wehr Technik und Beschaffung). Through an agreement with that agency, AFGL received data from five flights conducted in Germany by an instrumented DO-28 aircraft.

4.1 Instrumentation

The equipment on the DO-28 aircraft was described by Fuchs.²¹ In addition to instruments which measure temperature, humidity, pressure, and wind, the airplane had several instruments designed to measure drop-size distributions, liquid water content and ice accretion. The principal method of measuring drop-size distributions was to expose briefly an oil-coated slide to the outside air. The slide was then photographed through a microscope. As many as 80 such photographs were obtained on a given flight. Schickel²² compiled data from several of these flights.

Instruments specifically designed to measure icing included a Normalair-Garret heated rod system, in which a 1-cm thick rod extending from the surface of the airplane can be heated. An observer inside the aircraft activates the heater when a 2-cm thick ice layer has formed on the rod. This system can also give an estimate of liquid water content by noting how much energy is required to keep the rod de-iced.

On some flights a Rosemount Icing Detector similar to the one used on AFGL icing flights was available.

4.2 Results

In most cases the flights were in stratocumulus clouds, at altitudes of about 5,000 ft (1.5 km). Flight No. 47 on 22 February 1979, provided the typical profile shown in Figure 30. The 3- and 4-letter abbreviations are references to cities

21. Fuchs, W. (1978) Messung, Darstellung, and Auswertung meteorologischer Vereisungsparameter, Berichte Fliegergeophysikalischen Beratungsdienst der Bundeswehr, Nr. 23, Amt. für Wehrgeophysik, Traben-Trarbach, W. Germany, 35 pp.

22. Schickel, K. P. (1979) Ergebnisse der Auswertung von Tropfen-Impaktor Bildern aus vereisungsverdächtigen Stratuswolken, Deutsche Forschungsinstitut für Luft und Raumfahrt, IB nr 553-80-7, Oberpfaffenhofen, W. Germany, 95 pp.

along the route. Fuchs and Kaluza²³ further describe the weather encountered on this flight. On this particular flight, the aircraft experienced icing almost continuously as indicated by both the Rosemount Icing Detector and the heated rod.

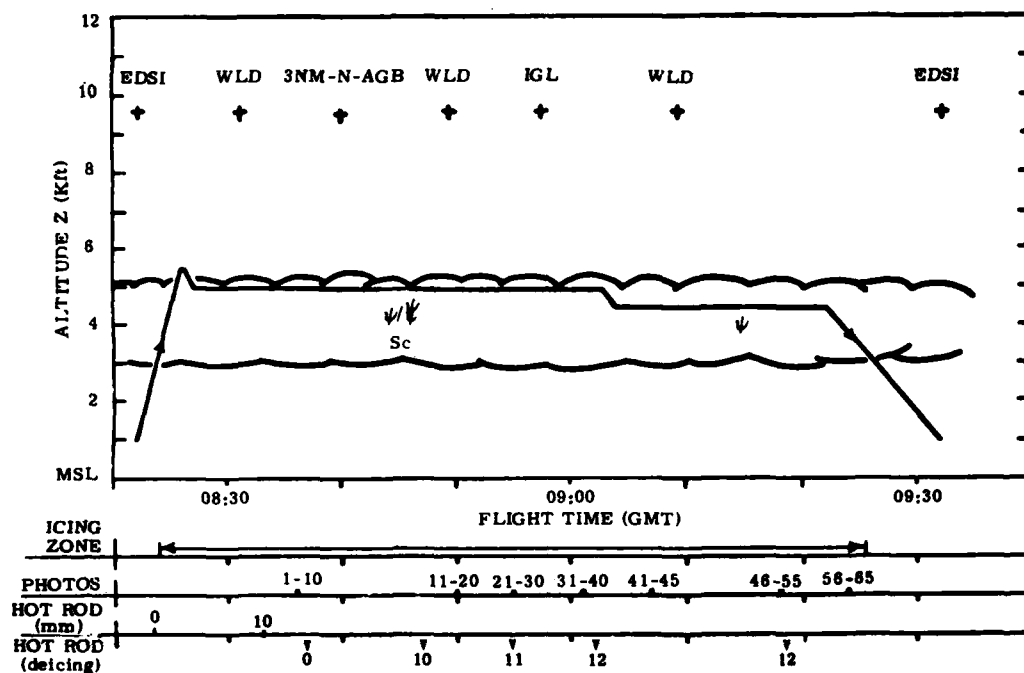


Figure 30. Profile of Flight Test No. 47, 22 February 1979. Solid black line represents the altitude of the aircraft. Light short curved lines indicates the cloud layer. Letters near top represent locations. The short downward pointing arrows indicate time of manual de-icing of the Hot Rod. The aircraft experienced light to moderate rime icing until its slight descent at 09:03. It then continued to experience light icing until it left the cloud deck

23. Fuchs, W., and Kaluza, J. (1980) Auswertung der Messflüge unter verisungsbedingungen, erprobungsstelle 61 d. BW Geophys BST/Desernat 234 Manching, W. Germany, 91 pp.

Over fifty oil-coated slides were exposed during this flight. Most of the droplets observed were 50 μm or less in diameter, although occasionally larger droplets were seen, the largest being over 100 μm in diameter. In most cases, there were relatively few small drops (less than 10 μm in diameter) and a larger number of droplets in the 15-30 μm range. This agrees with the observations made during the AFGL flights. In each of the four flights for which droplet distributions and reported icing were compared, a similar pattern, in which the majority of the droplets were larger than 10 μm in diameter, was observed. In a different case (Flight No. 28, on 13 December 1977), particles less than 3 μm in diameter were most frequently observed.

Thus, the data observed by both the German groups and AFGL seems to fit the same pattern reported by others; the droplets which are associated with icing are those which peak between 10 and 50 μm .

5. PROJECT SUMMARY

On Flight E79-50, 11 December 1979 by the AFGL's instrumented aircraft, the data showed the maximum icing rates recorded by the Rosemount Icing Meter, to have occurred during three small sections of Pass No. 7 near the top of cloud layer No. 2. These maximum icing cycles occurred during the time spans from 24:41:05 to 24:41:18, from 24:42:01 to 24:42:14 and from 24:42:23 to 24:42:36 and all three had icing cycles of 14 sec, equivalent to an icing rate of 2.18 mm/min. During these same time spans, the PMS ASSP produced maximum particle mode diameters of close to 12 μm , the JW LWC probe produced maximum values of approximately 0.68 g/m³ and the droplet concentration registered a relatively low averaged value of 335/cm³, compared to a value of 381/cm³ for Pass No. 6. See Figure 31 for the averaged values of these parameters corresponding to the maximum icing periods. Based on these limited data, it is suggested that the maximum icing rates occur near cloud top and that icing rates tend to increase with increases in mode diameter and LWC values.

An AFGL study by Glass and Grantham¹² examined the accuracy of the MC-130E cloud physics research aircraft's instrumentation concerned with icing measurements. Procedures for zero calibrating these instruments were developed. Comparison of liquid water measurements from the JW and from the ASSP indicated that these data were highly correlated and similar in magnitude. The analysis also showed that the Rosemount Ice Detector is a sensitive indicator of the fluctuations of liquid water in clouds with LWC not exceeding 0.8 g/m³. An AFGL study¹¹ has examined the problem of forecasting icing. Aircraft icing data were gathered by flying the MC-130E cloud physics research aircraft into areas in which icing was

was forecast. The degree of icing was recorded both by a human observer and by a Rosemount Ice Detector. Records from 25 flights were used. The results of these two types of observations of icing taken during the flight program were compared to the predicted results indicated by two forecast methods, the SKT and the AFGWC. The result of this comparison showed that there is considerable room for improvement in forecasting methods. Mechanical techniques, such as the Skew-T method, tend to overforecast the intensity of icing as observed by the Mission Director.

This AFGL icing study has noted a connection between droplet size and the icing rate. It would be useful to establish a relation between potential droplet size and some parameter available to a duty forecaster. This would involve further studies of the microphysics of supercooled clouds as well as an identification of synoptic features which could predict the droplet size distribution present in a given cloud.

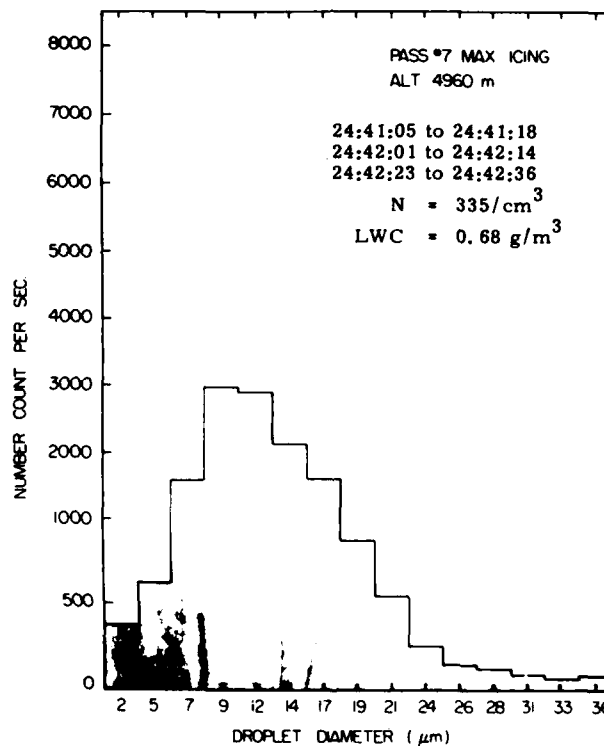


Figure 31. Averaged ASSP Measured Droplet Spectra for the Maximum Icing Rate in Sections of Pass No. 7

5.1 Recommendations

The study of layer type icing clouds associated with an approaching cold front offers many advantages to an in situ cloud measurement program. For example, the general locale for all of the measurements can be selected so that maximum ground support is available. Ground support should be in the form of rawinsonde launched on request, cloud radar coverage with Ka or Ku-band radar or lidar, and radio communication facilities. The Mission Director should arrange to take his airborne measurement during the formative stages of cloud development as well as after. On the MC-130 missions, the AFGL McIDAS satellite pictures were used on a real-time basis to direct the aircraft into areas of interest. Such general guidance plus high resolution radar, instrument and visual data should make it possible to sample all stages of cloud development. The airborne measurements should be performed systematically by three completely instrumented aircraft, that is, with measurement equipment similar to the MC-130E aircraft plus means of measuring the changes in vertical velocity encountered within the cloud.

Complete and accurate measurements, time and space correlated, taken in this manner would eliminate some of the problems presented by the data measurements of the 11 December 1979 mission.

The observed droplet size distributions were not compared with the simulated outputs from any dynamical cloud models, due to the unstructured nature of the measurements, however, significant processes and trends were noted. Data well organized in time and space could be used to test, study and perfect a stratocumulus cloud model.

Measurements of cloud droplet distributions and liquid water content are critical to the investigation of microphysical processes contributing to aircraft icing. The operating characteristics of these instruments should be known precisely. We therefore recommend that the users of cloud LWC measurements come together to plan and arrange for the design and development of a device capable of calibrating LWC instruments to known standards.

References

1. Bragg, M.B. (1981) Rime Ice Accretion and Its Effect on Airfoil Performance, PhD thesis, University of Ohio, 178 pp.
2. Hansman, R.J., and Hollister, W. (1981) Microwave Ice Prevention, Joint University Program for Air Transportation Research - 1981, NASA Conference Publication 2224, pp 39-51.
3. Hansman, R.J. (1982) The Interaction of Radio Frequency Electromagnetic Fields With Atmospheric Water Droplets With Applications to Aircraft Ice Prevention, FTL report R82-5, MIT Department of Aeronautics and Astronautics Flight Transportation Lab, 191 pp.
4. Sayward, J.M. (1979) Seeking Low Ice Adhesion, U.S. Army Cold Regions Research and Engineering Laboratory, Hanover, New Hampshire, Special Report 79-11, 88 pp.
5. Reinman, J.J., Shaw, R.J., and Olsen, W.A., Jr. (1982) Aircraft Icing Research at NASA, NASA Technical Memorandum 82-919, 15 pp.
6. Politovich, M.K. (1982) Characteristics of Icing Conditions in Winter-time Stratiform Clouds, Proceedings Conference on Cloud Physics, Chicago, Illinois, Amer. Meteor. Soc., 14-18 November 1982, pp 404-407.
7. Politovich, M.K. (1982) Microphysical Influences on Aircraft Icing, Proceedings, Conference on Cloud Physics, Chicago, Illinois, Amer. Meteor. Soc., 14-18 November 1982, pp 420-423.
8. Masters, C.O. (1983) A New Characterization of Supercooled Clouds Below 10,000 ft, Federal Aviation Administration Technical Center, Atlantic City Airport, New Jersey, DOT/FAA/CT-83-22, 21 pp.
9. Jeck, R.K. (1982) 5500 Miles of Liquid Water and Dropsizes Measurements in Supercooled Clouds Below 10,000 ft, Proceedings, Conference on Cloud Physics, Chicago, Illinois, Amer. Meteor. Soc., 14-18 November 1982, pp 408-411.
10. Barnes, A.A., Jr., Cohen, I.D., and McLeod, D.W. (1982) Investigations of Large Scale Storm Systems, Final Report, AFGI-TR-82-0169, AD A119862, 44 pp.

References

11. Cohen, I. D. (1983) Analysis of AFGL Aircraft Icing Data, AFGL-TR-83-0170, AD A137197.
12. Glass, M., and Grantham, D. D. (1981) Response of Cloud Microphysical Instruments to Aircraft Icing Conditions, AFGL-TR-81-0192, AD 112317.
13. Glass, M. (1982) Droplet Spectra and Liquid Water Content Measurements in Aircraft Icing Environments. Preprints, Conference on Cloud Physics Chicago, Illinois, Amer. Meteor. Soc., 14-18 November 1982, pp 400-403, AFGL-TR-82-0344, AD A122516.
14. Cohen, I. D. (1983) Preliminary Results of the AFGL Icing Study. Preprints, 9th Conference on Aerospace and Aeronautical Meteorology, Omaha, Nebraska, Amer. Meteor. Soc., 6-9 June 1983, pp 79-84, AFGL-TR-83-0147, AD A129843.
15. Ludwig, F. L., and Robinson, E. (1970) Observations of aerosols and droplets in California stratus. Tellus. 22:92-105.
16. Kunkel, B. A. (1982) Microphysical Properties of Fog at Otis AFB, AFGL-TR-820026, AD A119928.
17. Ide, R. F., and Richer, G. P. (1984) Comparison of Icing Cloud Instruments for 1982-1983 Icing Season Flight Program. NASA-TM-83569; E-1950; NAS 115:83569; USAAVSCOM-TR-84-C-1, 19 pp.
18. Baumgardner, D. (1983) An analysis and comparison of five water droplet measuring instruments. J. Appl. Meteor. 22:891-910.
19. Mason, B. J., and Chien, C. W. (1962) Cloud-droplet growth by condensation in cumulus, Quart. J. R. Met. Soc. 88:136.
20. Lee, I. Y., Hanel, G., and Pruppacher, H. R. (1980) A numerical determination of the evolution of cloud drop spectra due to condensation on natural aerosol particles, J. Atmos. Sci. 37(No. 8):1839.
21. Fuchs, W. (1978) Messung, Darstellung, and Auswertung meteorologischer Vereisungsparameter, Berichte Fuiden Geophysicalischen Beratungsdienst der Bundeswehr, Nr. 23, Amt. Fur Wehrgeophysik, Traben-Trarbach, W. Germany, 35 pp.
22. Schickel, K. P. (1979) Ergebnisse der Auswertung von Tropfen-Impaktor Bildern aus vereisungsverdachtigen Stratuswolken, Deutsche Forschungen and Versuchsanstalt Fur Luft und Raunfahrt, IB nr 553-80-7, Oberpfaffenhoffen, W. Germany, 95 pp.
23. Fuchs, W., and Kaluza, J. (1980) Auswertung der Messfluge unter vereisungsbedingungen, erprobungsstelle 61 d. BW Geophys BST/Desernat 234 Manching, W. Germany, 91 pp.

LIST OF ABBREVIATIONS

1. AFGL - Air Force Geophysics Laboratory
2. AFGWC - Air Force Global Weather Center Forecast Method
3. AFOSR - Air Force Office of Scientific Research
4. ASSP - PMS Axially Scattering Spectrometer Probe
5. BWB - Bundesamt Fur Wahr Technik und Beschaffung
6. EOARD - European Office of Aerospace Research and Development
7. FNT - Flint, Michigan
8. FRG - Federal Republic of Germany
9. GMT - Greenwich Mean Time
10. GSO - Greensboro, North Carolina
11. ΔH - Cloud depth in height
12. ICD - Average Number of Cycles of Rosemount Icing Detector
13. JW - Johnson-Williams hot wire liquid water content meter
14. LWC - Liquid Water Content
15. McIDAS - Man Computer Interactive Data Acquisition System
16. N - Particle number concentration (cm^{-3})
17. PMS - Particle Measuring System
18. R. H. - Relative Humidity
19. SKT - Skew-T Forecast Method
20. T. T. - Total Temperature
21. VIS - Visual Observation of Icing
22. WSO - Weather Service Office
23. Z - Greenwich Mean Time
24. 1-D - PMS one-dimensional probe
25. 2-D - PMS two-dimensional probe

END

FILMED

11-85

DTIC